
Dispelling the Curse of Singularities in Neural Network Optimizations

Hengjie Cao¹ Mengyi Chen^{1,*} Yifeng Yang^{1,*} Fang Dong¹ Ruijun Huang¹
 Anrui Chen¹ Jixian Zhou¹ Mingzhi Dong² Yujiang Wang³ Dongsheng Li⁴
 Wenyi Fang⁵ Yuanyi Lin⁵ FAN WU⁵ Li Shang^{1,†}

¹ Fudan University ² University of Bath ³ Oxford Suzhou Centre for Advanced Research
⁴ Microsoft Research Asia, Shanghai, China ⁵ Huawei

Abstract

This work investigates the optimization instability of deep neural networks from a less-explored yet insightful perspective: the emergence and amplification of singularities in the parametric space. Our analysis reveals that parametric singularities inevitably grow with gradient updates and further intensify alignment with representations, leading to increased singularities in the representation space. We show that the gradient Frobenius norms are bounded by the top singular values of the weight matrices, and as training progresses, the mutually reinforcing growth of weight and representation singularities, termed the curse of singularities, relaxes these bounds, escalating the risk of sharp loss explosions. To counter this, we propose Parametric Singularity Smoothing (PSS), a lightweight, flexible, and effective method for smoothing the singular spectra of weight matrices. Extensive experiments across diverse datasets, architectures, and optimizers demonstrate that PSS mitigates instability, restores trainability even after failure, and improves both training efficiency and generalization.

1 Introduction

Training instability, often manifesting as sudden loss explosions or erratic fluctuations, remains a long-standing and critical challenge in deep neural network (DNN) optimization [31, 9]. These instabilities frequently arise without early warning signals and can occur at any stage of training [24, 34], often leading to catastrophic collapse of the learning process. As a result, developing a stable training configuration is labor-intensive and error-prone: even small modifications in model architecture, optimizer, or data can undermine trainability and necessitate costly re-training. This problem is especially severe in large-scale foundation models [44], where each training run consumes weeks of computational time on thousands of GPUs. In these contexts, repeated instability-driven failures hinder iterative development, making a stable and restart-free training approach crucial.

Existing methods to address instability are largely empirical, e.g., gradient clipping [37, 28], and are sensitive to hyperparameter choices, often either failing to prevent divergence or excessively constraining learning dynamics [43, 8]. While theoretical insights link instabilities to sharp loss landscapes characterized by large Hessian eigenvalues [13, 25], the high complexity of loss landscape limits previous analyses from fully revealing the underlying mechanism of training instability.

In this work, we analyze training instability through the lens of growing singularities in the parametric space, a less-investigated perspective. Empirical investigations reveal that, across layers, the weight matrices, such as the query and key matrices in Transformers [39], become increasingly singular as training progresses, consistent with recent findings [29, 41]. More strikingly, we find that imminent

*Co-first authors.

catastrophic loss explosions are preceded by rapidly escalating singularities in both the parameter space and the representation space, characterized by growing rank deficiencies [11, 30].

These phenomena exhibit a mutually reinforcing trend: growing singularities in weight matrices lead to more degenerate representations, which in turn reinforce the singularity of subsequent gradient updates. This feedback loop culminates in a self-amplifying mechanism that triggers sharp, unrecoverable loss spikes. We term this failure mode *the curse of singularities*, a fundamental yet previously underexplored cause of optimization instability in DNNs.

To substantiate these observations, we adopt a simplified one-layer Transformer model and provide analysis grounded in the QK-gradient approximation [4]. We prove that the stable rank [35] (a soft surrogate for matrix rank) of weight matrices is provably lower-bounded to increase following each gradient update. Furthermore, we show that alignment between weight and representation singular vectors becomes tighter after backpropagation, further increasing representational singularity and reinforcing the instability. Crucially, we demonstrate that the Frobenius norm of gradients is bounded by the top singular value of the weight matrices, which means as the network becomes more singular, it also becomes more susceptible to large, unstable gradient updates. This dynamic relaxation of gradient norm bounds provides a mechanistic link between the growing singularities and sharp loss landscapes observed in prior work [13, 25].

Motivated by these findings, we introduce *Parametric Singularity Smoothing (PSS)*, a lightweight and adaptable technique that regularizes the singular value spectra of weight matrices during training. PSS proactively mitigates the mutual reinforcement of singularities, effectively restoring trainability even after instability onset. Empirical evaluations across diverse models, datasets, and optimization methods demonstrate that PSS consistently prevents training collapses, improves convergence efficiency, enhances generalization performance, and can restore trainability even after the occurrence of perceivable instabilities.

Our contributions are summarized as follows:

- We identify a mutually reinforcing growth of singularities in weight and representation matrices, termed the *curse of singularities*, as a primary cause of training instability in deep neural networks.
- We provide analysis on a simplified Transformer model, showing how gradient updates amplify parametric singularities and destabilize training.
- We propose Parametric Singularity Smoothing, a lightweight and effective method that mitigates singularity buildup and prevents loss explosions across diverse models and tasks.

2 Analysis

We begin with preliminary knowledge and notations. Next, we empirically demonstrate rank collapse in representation and parametric spaces, termed the curse of singularities, and explore its mechanism using a simplified one-layer transformer, providing key insights. Finally, we link singularity amplification to training instability.

2.1 Preliminaries

This section outlines key definitions, assumptions, and a one-layer transformer framework, forming the foundation for our subsequent analysis.

2.1.1 Definitions and Assumptions

We introduce the Stable Rank (SR) [35] to quantify parametric singularities. For a weight matrix $\mathbf{W} \in \mathbb{R}^{m \times d}$, we perform Singular Value Decomposition (SVD) to obtain singular values $\{\sigma_i\}_{i=1}^{\min(m,d)}$, left singular vectors $\{\mathbf{u}_i\}_{i=1}^m \in \mathbb{R}^m$, and right singular vectors $\{\mathbf{v}_i\}_{i=1}^d \in \mathbb{R}^d$, such that $\mathbf{W} = \sum_{i=1}^{\min(m,d)} \sigma_i \mathbf{u}_i \mathbf{v}_i^\top$. Throughout the paper, we assume all singular values are sorted in descending order, namely $\sigma_1 \geq \sigma_2 \geq \dots \geq \sigma_r > 0$, and we denote the i -th singular value of \mathbf{W} as $\sigma_i(\mathbf{W})$.

Definition 2.1 (Parametric Singularity). *The parametric singularity of a matrix \mathbf{W} is its stable rank, defined as the ratio of the squared Frobenius norm $\|\mathbf{W}\|_F^2$ to the squared spectral norm $\|\mathbf{W}\|_2^2$:*

$$\text{SR}(\mathbf{W}) = \frac{\|\mathbf{W}\|_F^2}{\|\mathbf{W}\|_2^2} = \frac{\sum_{i=1}^r \sigma_i^2}{\sigma_1^2}. \quad (1)$$

SR provides a smoothed measure of matrix rank, reflecting weight matrix singularity. A low SR indicates a pronounced singularity, where a few singular vectors dominate the parametric space.

Similarly, we define the singularity in the representation space. Let $\mathbf{X} = [\mathbf{x}_1, \mathbf{x}_2, \dots, \mathbf{x}_T] \in \mathbb{R}^{T \times d}$ represent an input of T tokens, each a d -dimensional vector ($T > d$). The expected input representation is $\mathbf{Z} = \mathbb{E}_{\mathcal{D}}[\mathbf{x}_1, \mathbf{x}_2, \dots, \mathbf{x}_T] \in \mathbb{R}^{T \times d}$, where the expectation is over the dataset \mathcal{D} .

Definition 2.2 (Representation Singularity). *For the SVD of $\mathbf{Z} = \sum_{i=1}^d \mu_i \boldsymbol{\alpha}_i \boldsymbol{\beta}_i^\top$, with singular values $\{\mu_i\}$, left singular vectors $\{\boldsymbol{\alpha}_i\}$, and right singular vectors $\{\boldsymbol{\beta}_i\}$, the representation singularity is:*

$$\text{SR}(\mathbf{Z}) = \frac{\|\mathbf{Z}\|_F^2}{\|\mathbf{Z}\|_2^2} = \frac{\sum_{i=1}^r \mu_i^2}{\mu_1^2}. \quad (2)$$

Owing to the long-tail feature distribution in the training set [1], the representation space exhibits significant singularity at the start of training. This is evidenced by an initial $\text{SR}(\mathbf{Z})$ below 20, as shown in Figure 1(b), and by the singular value distribution of the representation matrix, where the leading singular value μ_1 dominates the spectrum, as detailed in Appendix E.1.

To investigate the relationship between singularities in parametric and representation spaces, we quantify their alignment by measuring the cosine similarity between the top singular vectors, which represent the dominant directions due to pronounced singularities in both spaces.

Definition 2.3 (Singularity Alignment). *For matrices $\mathbf{W} \in \mathbb{R}^{m \times d}$ and $\mathbf{Z} \in \mathbb{R}^{T \times d}$, with top right singular vectors \mathbf{v}_1 and $\boldsymbol{\beta}_1$, respectively, the singularity alignment ϕ is defined as:*

$$\phi = \langle \mathbf{v}_1, \boldsymbol{\beta}_1 \rangle. \quad (3)$$

Empirical results in Fig. 1 show ϕ ranges between 0.6 and 1.0. For analytical simplicity, we assume ϕ approaches 1, with Appendix B confirming our theorems hold for empirical values.

Assumption 2.1 (Strong Singularity Alignment). *The top singular vectors are strongly aligned, satisfying $\mathbf{v}_1^\top \boldsymbol{\beta}_1 = \sqrt{1 - \epsilon}$, $\max_{r \geq 2} |\mathbf{v}_1^\top \boldsymbol{\beta}_r| \leq \sqrt{\epsilon}$, and $\epsilon \rightarrow 0$.*

In the expected representation space $\mathbf{Z} = \mathbb{E}[\mathbf{X}]$, the right singular vectors $\{\boldsymbol{\beta}_t\}_{t=1}^d$ of \mathbf{Z} form semantic bases, with singular values $\{\mu_t\}_{t=1}^d$ reflecting their prominence. To model token representations in this singular space, we introduce the following assumption:

Assumption 2.2 (Semantic Basis Composition). *Each token representation $\mathbf{x}_i \in \mathbf{X}$ is a linear combination of these bases, $\mathbf{x}_i = \sum_{t=1}^d c_{i,t} \boldsymbol{\beta}_t$, where the coefficients satisfy $\mathbb{E}[c_{i,t}] = \mu_t$.*

2.1.2 One-Layer Transformer and Gradient Approximation for the QK Matrix

Following the configuration outlined in [4], we adopt a one-layer Transformer, without loss of generality, to derive the gradient of the query-key parameter matrix for our analysis of the curse of singularities.

Softmax Approximation. To facilitate gradient derivation, we approximate the softmax function using a piecewise linear approach [4]. For a T -dimensional Key-Query inner product input $\boldsymbol{\omega} := \frac{\mathbf{X} \mathbf{W}_{QK} \mathbf{x}_T^\top}{\sqrt{d}} \in \mathbb{R}^T$, where $\mathbf{X} \in \mathbb{R}^{T \times d}$ is a sequence input with T tokens and \mathbf{W}_{QK} is query-key parameter matrix, the softmax is defined as $S(\boldsymbol{\omega})_i := \frac{\exp(\omega_i)}{\sum_{j=1}^T \exp(\omega_j)}$ for $i \in [T]$, mapping the i -th element of $\boldsymbol{\omega}$, denoted as ω_i , to the $[0, 1]$ interval. We employ a Taylor expansion around the origin, with coefficients $\gamma^i := \nabla_i S(\mathbf{0}) = \frac{1}{T} \mathbf{e}^i - \frac{1}{T^2} \mathbf{1}$ and $\gamma_0^i := S(\mathbf{0})_i = \frac{1}{T}$, where \mathbf{e}^i is the i -th one-hot vector and $\mathbf{1}$ is the all-ones vector. Thus, $\gamma_0^i = \frac{1}{T} - \frac{1}{T^2}$ and $\gamma_a^i = -\frac{1}{T^2}$ for $a \in [T] \setminus \{i\}$. To stabilize the approximation, we apply a truncation strategy with a fixed threshold c . When the absolute value of the approximation term exceeds c , the slope is clipped to 0:

$$\tilde{\gamma}_i^i = \begin{cases} \frac{T-1}{T^2}, & \text{if } \gamma_0^i \omega_i + \frac{1}{T} \gamma_0^i \in [-c, c] \\ 0, & \text{otherwise} \end{cases} \quad \tilde{\gamma}_a^i = \begin{cases} -\frac{1}{T^2}, & \text{if } \gamma_a^i \omega_a + \frac{1}{T} \gamma_0^i \in [-c, c] \\ 0, & \text{otherwise} \end{cases}$$

The resulting approximation in vector form is: $S(\omega) \approx \tilde{S}(\omega) = \Gamma^\top \omega + \tilde{\gamma}_0$, where $\Gamma := [\tilde{\gamma}^1, \tilde{\gamma}^2, \dots, \tilde{\gamma}^T]$ and $\tilde{\gamma}_0 = [\tilde{\gamma}_0^1, \tilde{\gamma}_0^2, \dots, \tilde{\gamma}_0^T]^\top$.

Model and Training Task. Next, we consider a one-layer transformer, simplifying the feed-forward network by assuming an identity activation function and omitting layer normalization. With $\mathbf{X} \in \mathbb{R}^{T \times d}$ as a sequence input with T tokens. Using the approximated softmax \tilde{S} , the output of a transformer with an attention layer A and a feedforward layer F is given by:

$$F(A(\mathbf{X}))_T = \mathbf{W}_F \left(\mathbf{W}_V \mathbf{X}^\top \tilde{S}(\omega) + \mathbf{x}_T \right) = \mathbf{W}_F \left(\mathbf{W}_V \mathbf{X}^\top \Gamma^\top \omega + \mathbf{W}_V \mathbf{X}^\top \tilde{\gamma}_0 + \mathbf{x}_T \right),$$

where $\mathbf{W}_F := \mathbf{W}_{F_2} \mathbf{W}_{F_1} + \mathbf{I}$, with $\mathbf{W}_{F_1}, \mathbf{W}_{F_2} \in \mathbb{R}^{d \times d}$ as feed-forward parameters. The query-key parameter matrix $\mathbf{W}_{QK} := \mathbf{W}_Q^\top \mathbf{W}_K \in \mathbb{R}^{d \times d}$ is optimized jointly, with \mathbf{W}_Q and \mathbf{W}_K constrained to be identical throughout training, ensuring \mathbf{W}_{QK} is treated as a unified parameter. The training task is causal language modeling, predicting the $(T + 1)$ -th token $\mathbf{y} := \mathbf{x}_{T+1} \in \mathbb{R}^d$ given T contextual tokens \mathbf{X} . The objective, using squared loss, is:

$$\mathcal{J}(\Theta) := \frac{1}{2} \mathbb{E} \|\mathbf{y} - F(A(\mathbf{X}))_T\|^2,$$

where Θ denotes model parameters, and the expectation is over the dataset.

QK-Gradient Approximation. For a sufficiently large sequence length T , the simplified gradient of the objective with respect to \mathbf{W}_{QK} [4] is:

$$\frac{1}{d} \sum_{i,j,a,b \in [T]} \mathbb{E} \left[\tilde{\gamma}_a^i \tilde{\gamma}_b^j P_{ij} (\mathbf{x}_b^\top \mathbf{W}_{QK} \mathbf{x}_T) \mathbf{x}_a \mathbf{x}_T^\top \right], \quad (4)$$

where $P_{ij} := (\mathbf{x}_i^\top \mathbf{W}_V^\top \mathbf{W}_F^\top \mathbf{W}_F \mathbf{W}_V \mathbf{x}_j)$ is independent of \mathbf{W}_{QK} , under the assumption that the other model parameters do not influence the analysis of the singularity of \mathbf{W}_{QK} .

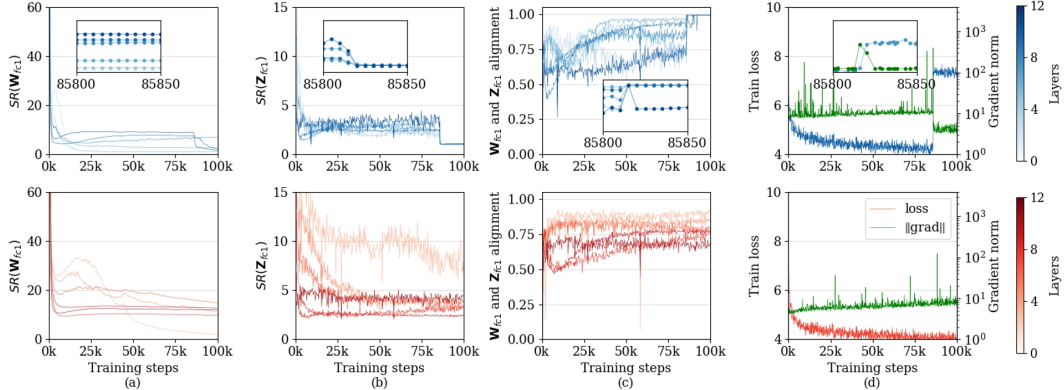


Figure 1: Evolution of $SR(\mathbf{W})$, $SR(\mathbf{Z})$, singularity alignment ϕ , and combined training loss (blue) and gradient norm (green, log scale) in the feedforward module (FFN) across 12 layers. The top panel shows unstable training ($LR=2e-4$), with a loss spike and sharp SR drop near step 85800, linking singularities to instability; the bottom panel shows stable training ($LR=1e-4$).

2.2 Unveiling the Curse of Singularities

Empirical results in Fig. 1(a)(b) illustrate the evolution of parametric singularity $SR(\mathbf{W})$ and representation singularity $SR(\mathbf{Z})$ during training. Both metrics exhibit a sharp decline early in training, stabilizing at low values with minor fluctuations thereafter. This trend is consistent across all network components, with additional module results provided in Appendix E. The singularity alignment ϕ , shown in Fig. 1(c), sharply increases early in training and remains high, indicating strong alignment between parametric and representation spaces. This alignment intensifies the mutual reinforcement of parametric and representation singularities, exacerbated by suboptimal hyperparameter settings like large learning rates, resulting in *the curse of singularities*.

Building on Section 2.1, we analyze a single-layer transformer under the assumptions to elucidate the mechanism driving the rank co-collapse phenomenon. We first demonstrate that parametric singularities inevitably increase after gradient updates.

Theorem 2.1 (Amplification of Parametric Singularity). *The gradient of the loss \mathcal{J} with respect to \mathbf{W}_{QK} amplifies parametric singularities, approximated as:*

$$\nabla_{\mathbf{W}_{QK}} \mathcal{J} = P \mathcal{O}(\sigma_1^2 \mu_1^2 \phi^2) \sum_{t=1} \mu_t^2 \boldsymbol{\beta}_t \boldsymbol{\beta}_t^\top, \quad (5)$$

where $P = \frac{1}{d} \sum_{i,j,a,b \in [T]} \mathbb{E} \left[\tilde{\gamma}_a^i \tilde{\gamma}_b^j P_{ij} \right]$ is negative and \mathcal{O} denotes the asymptotic order of the term. For large T and $\text{SR}(\mathbf{W}_K) > 1 + \frac{\text{SR}(\mathbf{Z})-1}{\phi^2}$, a gradient update with learning rate η reduces the stable rank of \mathbf{W}_Q and \mathbf{W}_K by:

$$\Delta \text{SR}(\mathbf{W}_Q) = \Delta \text{SR}(\mathbf{W}_K) = -\eta P \mathcal{O}(\mu_1^2 \phi^2) \mu_1^2 R, \quad (6)$$

where $R = [(1 - \text{SR}(\mathbf{W}_K)) \phi^2 + (\text{SR}(\mathbf{Z}) - 1)]$. This reduction drives $\text{SR}(\mathbf{W}_Q)$ and $\text{SR}(\mathbf{W}_K)$ toward $\text{SR}(\mathbf{Z})$, intensifying parametric singularities.

A detailed proof is provided in Appendix A.1. Given the dominance of μ_1 in Equation 5, gradient updates emphasize the dominant singular direction in the representation space. Strong alignment between the top singular vectors of the parametric and representation spaces causes these updates to disproportionately increase the largest singular values of \mathbf{W} , reducing $\text{SR}(\mathbf{W}_Q)$ and $\text{SR}(\mathbf{W}_K)$, an effect amplified by a large learning rate. This leads to stronger alignment between the two spaces, as demonstrated in the subsequent theorem.

Theorem 2.2 (Amplification of Singularity Alignment). *Let \mathbf{W}_{QK} be updated using the gradient $\nabla_{\mathbf{W}_{QK}} \mathcal{J}$ as in Equation 5. The singular alignment ϕ between \mathbf{W}_{QK} and \mathbf{Z} increases after the update. The change in alignment is given by:*

$$\Delta \phi = -\eta P \mathcal{O}(\sigma_1^2 \mu_1^2 \phi^2) \mu_1^2 \phi \sum_{k=2}^d \frac{(\mathbf{v}_k^\top \boldsymbol{\beta}_1)^2}{\sigma_1^2 - \sigma_k^2}, \quad (7)$$

indicating a positive update of ϕ .

A detailed proof is shown in Appendix A.2. The intuition behind the increase in alignment ϕ follows Theorem 2.1. Due to the prominence of μ_1 in the representation space, gradient updates primarily perturb the dominant direction \mathbf{v}_1 of the weight matrices toward $\boldsymbol{\beta}_1$, strengthening the alignment between \mathbf{v}_1 and $\boldsymbol{\beta}_1$, and thus enhancing singularity alignment.

Theorem 2.3 (Amplification of Representation Singularity). *We study the Key-Query inner product in a one-layer Transformer: $\mathbf{Z}_K^\top \mathbf{Z}_Q = \mathbf{Z} \mathbf{W}_{QK} \mathbf{Z}^\top$, then the stable rank of \mathbf{Z}_K and \mathbf{Z}_Q is:*

$$\text{SR}(\mathbf{Z}_K) = \text{SR}(\mathbf{Z}_Q) \approx 1 + \frac{[\text{SR}(\mathbf{W}_K) - 1] [\text{SR}(\mathbf{Z}) - 1]}{(d-1)\phi^2} \quad (8)$$

Let \mathbf{W}_{QK} be updated using the simplified gradient $\nabla_{\mathbf{W}_{QK}} \mathcal{J}$ as in Equation 5. Then if the following condition being satisfied: $\text{SR}(\mathbf{W}_K) > 1 + \frac{\phi^2 [\text{SR}(\mathbf{Z}) - 1]}{(d-1)^2}$, $\text{SR}(\mathbf{Z}_K)$ decreases.

A detailed proof is shown in Appendix A.3. Here, \mathbf{Z} represents the fixed input representation space in the one-layer Transformer setting. The output representation singularities are governed by $\text{SR}(\mathbf{W}_K)$ and singularity alignment ϕ , where a decreasing $\text{SR}(\mathbf{W}_K)$ or increasing ϕ reduces $\text{SR}(\mathbf{Z}_K)$ and $\text{SR}(\mathbf{Z}_Q)$, triggering rank co-collapse in parametric and representation spaces. In multi-layer models, shallow layer outputs feed deeper layers, propagating singularity reinforcement across layers and amplifying the *curse of singularities* spatially and temporally.

2.3 Singularity and Training Instability

The degree of singularity strongly correlates with the Frobenius norm of gradients, a key indicator of training stability. As shown in Figure 1(d), gradient norms rise with increasing singularity during training. Figure 1(top) illustrates a training failure, further highlighting this connection. Around step

85,800, the loss surges from 4 to 7, accompanied by a sharp gradient norm spike and a rapid increase in both parametric and representation singularities.

Building on prior foundations, we establish that the gradient Frobenius norm is both lower and upper bounded by parametric singularity. Since the proof of Theorem 2.1 shows that training simultaneously increases σ_1 while reducing $\text{SR}(\mathbf{W}_K)$, we use σ_1 as a proxy for the growing parametric singularity.

Theorem 2.4 (Bounds on Gradient Frobenius Norm). *The Frobenius norm of the QK-gradient $\nabla_{\mathbf{W}_{QK}} \mathcal{J}$ is bounded as follows:*

1. *Lower Bound: Assuming a fixed Frobenius norm $\|\mathbf{W}_{QK}\|_F^2 = \sum_{k=1}^d \sigma_k^2 = M > 0$ at a given step, the gradient norm satisfies:*

$$\|\nabla_{\mathbf{W}_{QK}} \mathcal{J}\|_F \geq K \alpha_1 \sigma_1^2(\mathbf{W}_{QK}), \quad (9)$$

where $K = P \cdot \|\sum_{t=1}^d \mu_t^2 \beta_t \beta_t^\top\| > 0$ and $\alpha_1 = \left(\sum_{r=1}^d \mu_r \cdot (\mathbf{v}_1^\top \beta_r) \right)^2$.

2. *Upper Bound:*

$$\|\nabla_{\mathbf{W}_{QK}} \mathcal{J}\|_F \leq C \sigma_1^2(\mathbf{W}_V) [\sigma_1(\mathbf{W}_{F_1}) \sigma_1(\mathbf{W}_{F_2}) + 1]^2 \sigma_1(\mathbf{W}_{QK}), \quad (10)$$

where $C = \frac{1}{d} \sum_{i,j,a,b \in [T]} \mathbb{E} [\tilde{\gamma}_a^i \tilde{\gamma}_b^j] \mathcal{O}(\mu_1^4 \phi^2) \text{SR}(\mathbf{Z})$.

A detailed proof is shown in Appendix A.4. As shown in Equation 19, the gradient norm’s lower bound increases with parametric singularity, driven by σ_1^2 . This trend, observed in both stable and unstable training regimes (Figure 1(d)), suggests that reducing the learning rate in later training stages is essential to accommodate larger gradients. Similarly, Equation 20 reveals that the upper bound grows rapidly with increasing parametric singularity, amplifying the risk of unstable gradient updates. Together, these dynamics—where gradient norm bounds relax with growing singularity—establish a mechanistic connection between parametric singularities and training instability.

3 Method

To stabilize DNN training, we propose Parametric Singularity Smoothing (PSS), a lightweight module that integrates seamlessly into DNNs. Using gradient norms as instability indicators, PSS smooths weight matrix singular spectra, reducing parametric singularities and tightening gradient norm bounds. Crucially, PSS preserves network performance and can restore trainability post-instability.

3.1 Design of PSS

Detection. Prior analyses has established a link between gradient norm spikes, heightened singularity, and training instability. We leverage gradient norms as early instability indicators, computed during backpropagation. We define the ratio $\mu_{t+1} = \frac{\|\mathbf{g}^{t+1}\|_F}{\|\mathbf{g}_{avg}^t\|_F}$, where \mathbf{g}^{t+1} is the gradient at step $t+1$, and $\mathbf{g}_{avg}^t = (1 - \alpha) \mathbf{g}_{avg}^{t-1} + \alpha \mathbf{g}^t$ is the exponentially weighted moving average of gradients, with smoothing coefficient α . If $\mu_{t+1} \geq \tau$, where τ is a threshold, potential instability is flagged, triggering a smoothing operation to curb parametric singularity growth. The choice of τ is robust: a lower τ may cause false positives without disrupting training, while a higher τ risks missing instabilities, yet PSS can still recover stability post-instability.

Protection. Upon detecting instability, we smooth the singular spectrum of the parameter matrix \mathbf{W} to curb gradient norm growth. For efficiency, we compute dominant singular values and vectors up to the matrix’s stable rank using the Power Iteration Method [16] for σ_1 and Dominant Direction Decomposition (DDD) [17] to obtain $\mathbf{W}_{dominant} = \sum_{i=1}^{\lfloor \text{SR}(\mathbf{W}) \rfloor} \sigma_i \mathbf{u}_i \mathbf{v}_i^\top$. We apply a smoothing function f_{smooth} to yield $\sigma^* = f_{smooth}(\sigma)$, reparameterizing as $\mathbf{W}_{dominant}^* = \sum_{i=1}^{\lfloor \text{SR}(\mathbf{W}) \rfloor} \sigma_i^* \mathbf{u}_i \mathbf{v}_i^\top$, resulting in $\mathbf{W}^* = \mathbf{W} - \mathbf{W}_{dominant} + \mathbf{W}_{dominant}^*$. The flexible f_{smooth} supports methods like Logarithmic Scaling, Softplus, Softmax, or clipping, preserving singular value order and increasing SR, with the choice tailored to the task.

3.2 Benefits of PSS

PSS is a lightweight module that seamlessly integrates into DNNs to detect and prevent instability without degrading performance. It can restore trainability post-instability while preserving all singular

Table 1: Stability test results for BERT-base and GPT-2-Medium. Entries follow the format x/y (z), where y indicates the total number of evaluations conducted, x reflects the count of instability instances observed during training, and z reports the final test loss.

Method \ Model	BERT-base			GPT-2-Medium		
	lr=1e-4	lr=2e-4	lr=4e-4	lr=5e-4	lr=1e-3	lr=4e-3
Naive	0/3 _{3.0} ±0.2	3/3 _{7.5} ±0.1	3/3 _{7.5} ±0.1	0/3 _{3.8} ±0.1	3/3 _{7.4} ±0.1	3/3 _{7.5} ±0.1
GC	0/3 _{2.9} ±0.1	0/3 _{2.7} ±0.1	3/3 _{7.4} ±0.1	0/3 _{3.7} ±0.1	0/3 _{3.9} ±0.1	3/3 _{7.5} ±0.1
OR	0/3 _{3.1} ±0.1	1/3 _{2.9} ±0.1	3/3 _{7.4} ±0.1	0/3 _{3.8} ±0.1	3/3 _{7.5} ±0.1	3/3 _{7.4} ±0.1
QK-Norm	0/3 _{3.0} ±0.1	0/3 _{2.7} ±0.1	0/3 _{2.8} ±0.1	0/3 _{3.8} ±0.1	0/3 _{3.9} ±0.1	3/3 _{7.2} ±0.4
PSS	0/3 _{3.0} ±0.1	0/3 _{2.8} ±0.1	0/3 _{2.6} ±0.1	0/3 _{3.8} ±0.1	0/3 _{4.0} ±0.1	0/3 _{4.5} ±0.1

vectors and their learned features. By smoothing the singular spectrum, PSS controls gradient norms and reduces excessive dominance of certain directions, allowing smaller ones to emerge. This enables progressive refinement of the singular value distribution during training.

4 Experiments

In this section, we evaluate the performance of Parametric Singularity Smoothing (PSS) through a series of experiments across various scenarios. Our primary goal is to demonstrate how PSS effectively preserves stability during training without degrading model performance. We also highlight its efficiency and lightweight nature, ensuring minimal computational overhead.

4.1 Experimental Setup

Configuration. We evaluate PSS across model scales (110M to 7B parameters) using BERT [10], GPT-2 [32], and Llama-3 [12], with primary results on BERT-base and GPT-2-Medium (larger models in Appendix D.3). Pretraining uses Wikitext [26] (BERT), Amazon-review/OpenWebText [15] (GPT-2), and English Wikipedia (Llama-3). Tests cover instability scenarios (learning rate, warmup, batch size) with comparisons to Gradient Clipping(GC), Orthogonal Regularization(OR) [6, 5], and Query-Key Normalization(QK-Norm) [20]. See Appendix D.1 for settings.

Evaluation. We assess PSS’s effectiveness by: (1) measuring loss explosion frequency across identical configurations [42], (2) evaluating expanded stable learning rate ranges and corresponding performance, and (3) comparing computational overhead [33] to highlight PSS’s efficiency. Results demonstrate PSS’s robustness in rescue time and smoothing policy choice, while downstream task performance confirms no model degradation.

4.2 Effectiveness in Preventing Instability

Stability Maintenance. To evaluate PSS’s stability, we compare it against three stabilization methods across various hyper-parameter settings, primarily learning rates. Each PSS-baseline comparison uses the same random seed to assess instability prevention, repeated with three distinct seeds for consistency. Additional tests on warmup steps and batch size are in Appendix D.4.

Table 1 shows GC and OR stabilize training only at low LRs, failing at higher LRs, while QK-Norm, though improved, falters at larger LRs. PSS consistently ensures stability across all settings and seeds. Appendix D.2 presents BERT-base test loss curves at LRs of 1e-4 and 4e-4, demonstrating PSS’s ability to mitigate loss explosions with minimal spikes and no extra recovery steps.

Model Performance. Fig. 2 compares final test loss across various LRs for BERT-base and GPT-2-Medium. PSS significantly expands the stable LR range, achieving up to a 10-fold increase compared to GC and OR. QK-Norm underperforms PSS at large LRs, particularly on GPT-2, where its loss surges with increasing LRs. For larger models (BERT-large, GPT-2-Large, GPT-2-XL), PSS extends the stable LR range by up to 5 times without sacrificing convergence, enhancing hyperparameter tuning flexibility.

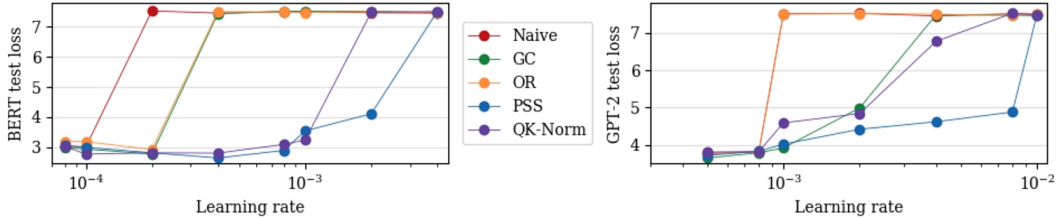


Figure 2: Final loss across LRs for each stabilization method (BERT-base left, GPT-2-Medium right).

4.3 Computational Efficiency of PSS

Table 2: Computational cost comparison of different methods in terms of floating-point (Fp) computations and execution time for both a single step and 100k steps.

Method	CPU+GPU cost @ 1 step		CPU+GPU cost @ 100k step	
	Fp cost (TFLOPs)	Time (ms)	Fp cost (PFLOPs)	Time (hours)
	9.33	781 ± 10	933	9.15 ± 0.08
Naive	9.33	784 ± 12	936	9.14 ± 0.10
GC	9.33	864 ± 15	1146	10.04 ± 0.10
OR	11.46	780 ± 23	1146	9.20 ± 0.13
QK-Norm	9.33	1979 ± 25	936	9.17 ± 0.09
PSS	9.36	1979 ± 25	936	9.17 ± 0.09

($m = 8192$, $n = 28672$, $b = 8192$), $k < 8192$ (exact k pending). Since $m, n \gg b$ and $\log k < k < \max(m, n)$, $\log k \approx b$, ensuring low overhead. Table 2 (“1 step” section) shows PSS increases CPU + GPU time by up to $2.40\times$ a baseline step.

Total Training Overhead. PSS incurs minimal overall overhead, activating on average in 0.1% of training steps, with a maximum below 0.25% (see Appendix D.5). This low frequency holds across model sizes and architectures, increasing slightly with larger learning rates due to more gradient spikes, showcasing PSS’s adaptability. Table 2 (“100k step” section) shows that training BERT-base with a large LR adds only 0.21% extra training time over the baseline, highlighting PSS’s efficiency.

4.4 Robustness of PSS

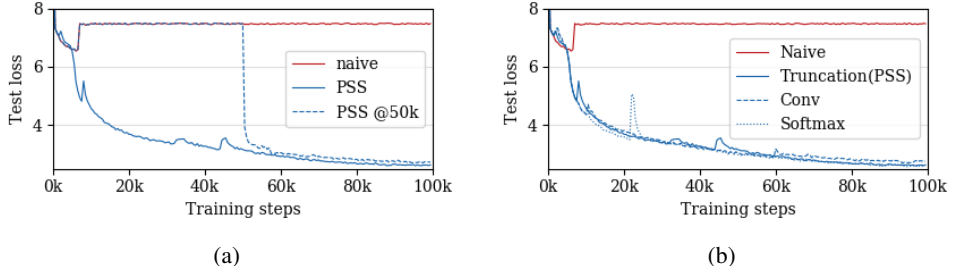


Figure 3: For BERT-base trained at a learning rate of $4\text{e-}4$: (a) Test loss curves comparing the unstable naive baseline with PSS applied at various stages. (b) Test loss curves using different smoothing policies upon instability detection.

PSS demonstrates robust performance across multiple critical dimensions:

Rescue Robustness. Fig. 3(a) shows PSS’s robustness across instability stages. Proactively applied, PSS induces only minor, transient loss spikes, averting future instability. Post-divergence, it quickly mitigates gradient vanishing and restores training. Unlike prior methods—often ineffective or reliant on slow trial-and-error or checkpoint recovery—PSS detects instability reliably: false positives don’t disrupt training, and it stabilizes even after full divergence, offering an efficient solution.

Smoothing Policy Robustness. As shown in Fig.3, PSS is effective across a variety of smoothing policies, all of which yield stable training outcomes. Further details on each smoothing policy are provided in AppendixC.1. This suggests that once parametric singularity is addressed, the specific choice of smoothing policy is less critical, emphasizing the method’s robustness in policy selection.

Compatibility Robustness. PSS is highly adaptable, requiring no specific model architecture, optimizer, or dataset. This ensures easy integration with minimal code changes. Moreover, PSS is orthogonal to existing stabilization techniques, complementing and enhancing them without conflict, further improving training stability.

4.5 Performance on Downstream Tasks

Comparable Accuracy. To evaluate PSS’s impact on model performance, we conduct experiments on four downstream tasks using BERT-base trained for 100k steps, as shown in Table 3. PSS not only ensures training stability but also achieves comparable or superior accuracy compared to the naive baseline, particularly at larger learning rates (LRs).

Benefits of Large LRs. Table 3 demonstrates that PSS with a large LR of 4e-4 achieves better loss and downstream accuracy in 70k steps compared to 100k steps at LR 1e-4. This indicates PSS reduces the training steps required at large LRs, lowering computational costs while unlocking the potential of higher LRs for improved performance.

Table 3: Downstream tasks on BERT-base.

Method	test loss	COLA (acc)	SST-2 (acc)	MRPC (acc)	MNLI (acc)	QNLI (acc)	RTE (acc)
Naive @ 100k steps(lr=1e-4)	3.05	50.8%	85.2%	82.4%	81.6%	84.3%	81.9%
PSS @ 100k steps(lr=1e-4)	2.95	51.9%	84.9%	83.3%	82.0%	85.0%	81.2%
PSS @ 100k steps(lr=2e-4)	2.78	51.6%	86.0%	83.4%	82.8%	85.8%	83.3%
PSS @ 100k steps(lr=4e-4)	2.64	52.2%	85.6%	84.8%	82.5%	85.8%	84.5%
PSS @ 70k steps(lr=2e-4)	2.92	51.0%	85.8%	81.7%	82.5%	83.7%	82.4%
PSS @ 70k steps(lr=4e-4)	2.84	52.3%	86.1%	84.6%	81.9%	85.4%	82.8%

5 Related Work

Training instability has been widely studied from a theoretical perspective. Techniques like meticulous weight initialization [14, 19, 27, 22] and normalization [3, 23, 38] are critical for stabilizing neural networks. Additionally, research has examined the effects of activation non-linearity [21], skip connections [36], and model depth and width [18, 40] on stability. In practice, gradient clipping [2] is a common method for managing instability by capping gradient magnitudes. Adaptive methods, such as those proposed by [37], improve on this by incorporating optimizers like Adagrad. Other approaches include selectively freezing parameters in ViT models [7] and using spectral normalization to prevent attention entropy collapse [42], further stabilizing training. Despite the aforementioned stability methods, models still encounter instability under large LRs, and these methods prove ineffective once instability arises. Our PSS method significantly broadens the usable LR range and ensures reliable training.

6 Conclusion

We expose the phenomenon of rank co-collapses in the parametric and representation spaces as *the curse of singularities* and deem it an essential cause for training instabilities. We thoroughly analyze the theoretical properties behind this curse and acquire several key findings. In light of those discoveries, we propose a method, Parametric Singularity Smoothing (PSS), to smooth the singular spectrum of the weight matrices when necessary, which could effectively prevent unstable training without compromising performance. More favourably, PSS could restore trainability even after perceivable instability. As a lightweight, generalized, flexible, and compatible module, PSS can

be integrated into various networks to save time and computation on undesired re-training, especially for large language models. Moreover, we open a new gate for analyzing the instability behaviour in the parametric space.

References

- [1] Reddit comments dataset. [https://clickhouse.com/docs/en/getting-started/example-datasets/reddit-comments,,](https://clickhouse.com/docs/en/getting-started/example-datasets/reddit-comments/) 2024.
- [2] Zeyuan Allen-Zhu, Yuanzhi Li, and Zhao Song. A convergence theory for deep learning via over-parameterization. In *International conference on machine learning*, pages 242–252. PMLR, 2019.
- [3] Jimmy Lei Ba, Jamie Ryan Kiros, and Geoffrey E Hinton. Layer normalization. *arXiv preprint arXiv:1607.06450*, 2016.
- [4] Han Bao, Ryuichiro Hataya, and Ryo Karakida. Self-attention networks localize when qk -eigenspectrum concentrates. *arXiv preprint arXiv:2402.02098*, 2024.
- [5] Andrew Brock. Large scale gan training for high fidelity natural image synthesis. *arXiv preprint arXiv:1809.11096*, 2018.
- [6] Andrew Brock, Theodore Lim, James Millar Ritchie, and Nicholas J Weston. Neural photo editing with introspective adversarial networks. In *5th International Conference on Learning Representations 2017*, 2017.
- [7] X Chen, S Xie, and K He. An empirical study of training self-supervised vision transformers. In *2021 IEEE/CVF International Conference on Computer Vision (ICCV)*, pages 9620–9629, 2021.
- [8] Xiangyi Chen, Steven Z. Wu, and Mingyi Hong. Understanding gradient clipping in private sgd: A geometric perspective. In H. Larochelle, M. Ranzato, R. Hadsell, M.F. Balcan, and H. Lin, editors, *Advances in Neural Information Processing Systems*, volume 33, pages 13773–13782. Curran Associates, Inc., 2020.
- [9] Aakanksha Chowdhery, Sharan Narang, Jacob Devlin, Maarten Bosma, Gaurav Mishra, Adam Roberts, Paul Barham, Hyung Won Chung, Charles Sutton, Sebastian Gehrmann, et al. Palm: Scaling language modeling with pathways. *Journal of Machine Learning Research*, 24(240):1–113, 2023.
- [10] Jacob Devlin, Ming-Wei Chang, Kenton Lee, and Kristina Toutanova. Bert: Pre-training of deep bidirectional transformers for language understanding, 2019.
- [11] Yihe Dong, Jean-Baptiste Cordonnier, and Andreas Loukas. Attention is not all you need: Pure attention loses rank doubly exponentially with depth. In *International Conference on Machine Learning*, pages 2793–2803. PMLR, 2021.
- [12] A. Grattafiori et al. The llama 3 herd of models. 2024.
- [13] Justin Gilmer, Behrooz Ghorbani, Ankush Garg, Sneha Kudugunta, Behnam Neyshabur, David Cardoze, George Edward Dahl, Zachary Nado, and Orhan Firat. A loss curvature perspective on training instabilities of deep learning models. In *International Conference on Learning Representations*, 2021.
- [14] Xavier Glorot and Yoshua Bengio. Understanding the difficulty of training deep feedforward neural networks. In *Proceedings of the thirteenth international conference on artificial intelligence and statistics*, pages 249–256. JMLR Workshop and Conference Proceedings, 2010.
- [15] Aaron Gokaslan and Vanya Cohen. Openwebtext corpus. <http://Skylion007.github.io/OpenWebTextCorpus>, 2019.
- [16] Gene H Golub and Charles F Van Loan. *Matrix computations*. JHU press, 2013.
- [17] Nathan Halko, Per-Gunnar Martinsson, and Joel A Tropp. Finding structure with randomness: Stochastic algorithms for constructing approximate matrix decompositions. *arXiv preprint arXiv:0909.4061*, 909, 2009.
- [18] Boris Hanin. Which neural net architectures give rise to exploding and vanishing gradients? *Advances in neural information processing systems*, 31, 2018.

[19] Kaiming He, Xiangyu Zhang, Shaoqing Ren, and Jian Sun. Delving deep into rectifiers: Surpassing human-level performance on imagenet classification. In *Proceedings of the IEEE international conference on computer vision*, pages 1026–1034, 2015.

[20] Alex Henry, Prudhvi Raj Dachapally, Shubham Pawar, and Yuxuan Chen. Query-key normalization for transformers, 2020.

[21] Kai Hu. Revisiting exploding gradient: A ghost that never leaves. *Revisiting_Exploding_Gradient.pdf*, 2016.

[22] Wei Hu, Lechao Xiao, and Jeffrey Pennington. Provable benefit of orthogonal initialization in optimizing deep linear networks. *arXiv preprint arXiv:2001.05992*, 2020.

[23] Sergey Ioffe and Christian Szegedy. Batch normalization: Accelerating deep network training by reducing internal covariate shift. In *International conference on machine learning*, pages 448–456. pmlr, 2015.

[24] Sekitoshi Kanai, Yasuhiro Fujiwara, and Sotetsu Iwamura. Preventing gradient explosions in gated recurrent units. *Advances in neural information processing systems*, 30, 2017.

[25] Hoki Kim, Jinseong Park, Yujin Choi, and Jaewook Lee. Stability analysis of sharpness-aware minimization. *arXiv preprint arXiv:2301.06308*, 2023.

[26] Stephen Merity, Caiming Xiong, James Bradbury, and Richard Socher. Pointer sentinel mixture models, 2016.

[27] Dmytro Mishkin and Jiri Matas. All you need is a good init. *arXiv preprint arXiv:1511.06422*, 2015.

[28] Igor Molybog, Peter Albert, Moya Chen, Zachary DeVito, David Esiobu, Naman Goyal, Punit Singh Koura, Sharan Narang, Andrew Poulton, Ruan Silva, Binh Tang, Diana Liskovich, Puxin Xu, Yuchen Zhang, Melanie Kambadur, Stephen Roller, and Susan Zhang. A theory on adam instability in large-scale machine learning, 2023.

[29] Alireza Mousavi-Hosseini, Sejun Park, Manuela Girotti, Ioannis Mitliagkas, and Murat A Erdogdu. Neural networks efficiently learn low-dimensional representations with sgd. *arXiv preprint arXiv:2209.14863*, 2022.

[30] Lorenzo Noci, Sotiris Anagnostidis, Luca Biggio, Antonio Orvieto, Sidak Pal Singh, and Aurelien Lucchi. Signal propagation in transformers: Theoretical perspectives and the role of rank collapse. *Advances in Neural Information Processing Systems*, 35:27198–27211, 2022.

[31] George Philipp, Dawn Song, and Jaime G Carbonell. The exploding gradient problem demystified-definition, prevalence, impact, origin, tradeoffs, and solutions. *arXiv preprint arXiv:1712.05577*, 2017.

[32] Alec Radford, Jeffrey Wu, Rewon Child, David Luan, Dario Amodei, Ilya Sutskever, et al. Language models are unsupervised multitask learners. *OpenAI blog*, 1(8):9, 2019.

[33] Jeff Rasley, Samyam Rajbhandari, Olatunji Ruwase, and Yuxiong He. Deepspeed: System optimizations enable training deep learning models with over 100 billion parameters. In *Proceedings of the 26th ACM SIGKDD International Conference on Knowledge Discovery & Data Mining*, pages 3505–3506, 2020.

[34] Antônio H Ribeiro, Koen Tiels, Luis A Aguirre, and Thomas Schön. Beyond exploding and vanishing gradients: analysing rnn training using attractors and smoothness. In *International conference on artificial intelligence and statistics*, pages 2370–2380. PMLR, 2020.

[35] Mark Rudelson and Roman Vershynin. Sampling from large matrices: An approach through geometric functional analysis. *Journal of the ACM (JACM)*, 54(4):21–es, 2007.

[36] Christian Szegedy, Sergey Ioffe, Vincent Vanhoucke, and Alexander Alemi. Inception-v4, inception-resnet and the impact of residual connections on learning. In *Proceedings of the AAAI conference on artificial intelligence*, volume 31, 2017.

- [37] Jiaxi Tang, Yoel Drori, Daryl Chang, Maheswaran Sathiamoorthy, Justin Gilmer, Li Wei, Xinyang Yi, Lichan Hong, and Ed H. Chi. Improving training stability for multitask ranking models in recommender systems. In *Proceedings of the 29th ACM SIGKDD Conference on Knowledge Discovery and Data Mining*, KDD '23, page 4882–4893, New York, NY, USA, 2023. Association for Computing Machinery.
- [38] Dmitry Ulyanov, Andrea Vedaldi, and Victor Lempitsky. Instance normalization: The missing ingredient for fast stylization. *arXiv preprint arXiv:1607.08022*, 2016.
- [39] Ashish Vaswani, Noam Shazeer, Niki Parmar, Jakob Uszkoreit, Llion Jones, Aidan N. Gomez, Łukasz Kaiser, and Illia Polosukhin. Attention is all you need. *Advances in Neural Information Processing Systems*, 2017.
- [40] Greg Yang and Sam S Schoenholz. Deep mean field theory: Layerwise variance and width variation as methods to control gradient explosion. 2018.
- [41] Emanuele Zangrando, Piero Deidda, Simone Brugiapaglia, Nicola Guglielmi, and Francesco Tudisco. Neural rank collapse: Weight decay and small within-class variability yield low-rank bias. *arXiv preprint arXiv:2402.03991*, 2024.
- [42] Shuangfei Zhai, Tatiana Likhomanenko, Eta Littwin, Dan Busbridge, Jason Ramapuram, Yizhe Zhang, Jiatao Gu, and Joshua M Susskind. Stabilizing transformer training by preventing attention entropy collapse. In *International Conference on Machine Learning*, pages 40770–40803. PMLR, 2023.
- [43] Jingzhao Zhang, Tianxing He, Suvrit Sra, and Ali Jadbabaie. Why gradient clipping accelerates training: A theoretical justification for adaptivity. In *International Conference on Learning Representations*, 2020.
- [44] Susan Zhang, Stephen Roller, Naman Goyal, Mikel Artetxe, Moya Chen, Shuohui Chen, Christopher Dewan, Mona Diab, Xian Li, Xi Victoria Lin, et al. Opt: Open pre-trained transformer language models. *arXiv preprint arXiv:2205.01068*, 2022.

Appendix

A Theoretical Proof.

A.1 Parametric Singularity Trend.

Theorem A.1 (Amplification of Parametric Singularity). *The gradient of the loss \mathcal{J} with respect to \mathbf{W}_{QK} amplifies parametric singularities, approximated as:*

$$\nabla_{\mathbf{W}_{QK}} \mathcal{J} = P \mathcal{O}(\sigma_1^2 \mu_1^2 \phi^2) \sum_{t=1}^d \mu_t^2 \boldsymbol{\beta}_t \boldsymbol{\beta}_t^\top, \quad (11)$$

where $P = \frac{1}{d} \sum_{i,j,a,b \in [T]} \mathbb{E} \left[\tilde{\gamma}_a^i \tilde{\gamma}_b^j P_{ij} \right]$ is negative. For large T and $\text{SR}(\mathbf{W}_K) > 1 + \frac{\text{SR}(\mathbf{Z})-1}{\phi^2}$, a gradient update with learning rate η reduces the stable rank of \mathbf{W}_Q and \mathbf{W}_K by:

$$\Delta \text{SR}(\mathbf{W}_Q) = \Delta \text{SR}(\mathbf{W}_K) = -\eta P \mathcal{O}(\mu_1^2 \phi^2) \mu_1^2 R, \quad (12)$$

where $R = [(1 - \text{SR}(\mathbf{W}_K)) \phi^2 + (\text{SR}(\mathbf{Z}) - 1)]$. This reduction drives $\text{SR}(\mathbf{W}_Q)$ and $\text{SR}(\mathbf{W}_K)$ toward $\text{SR}(\mathbf{Z})$, intensifying parametric singularities.

Proof. Through semantic basis composition, the token representations \mathbf{x}_a , \mathbf{x}_b , and \mathbf{x}_T in Equation 4 can be expressed as linear combinations of the semantic basis vectors:

$$\mathbf{x}_a = \sum_{i=1}^d c_{a,i} \boldsymbol{\beta}_i, \mathbf{x}_b = \sum_{i=1}^d c_{b,i} \boldsymbol{\beta}_i, \mathbf{x}_T = \sum_{i=1}^d c_{T,i} \boldsymbol{\beta}_i$$

Substituting this into Equation 4 gives the semantic feature decomposition form of the QK -gradient $\nabla_{\mathbf{W}_{QK}} \mathcal{J}$.

$$\begin{aligned} \nabla_{\mathbf{W}_{QK}} \mathcal{J} &= \frac{1}{d} \sum_{i,j,a,b \in [T]} \mathbb{E} \left[\tilde{\gamma}_a^i \tilde{\gamma}_b^j P_{ij} (\mathbf{x}_b^\top \mathbf{W}_{QK} \mathbf{x}_T) \mathbf{x}_a \mathbf{x}_T^\top \right] \\ &= \frac{1}{d} \sum_{i,j,a,b \in [T]} \mathbb{E} \left[\tilde{\gamma}_a^i \tilde{\gamma}_b^j P_{ij} \left(\sum_{r=1}^d c_{b,r} \boldsymbol{\beta}_r^\top \right) \mathbf{W}_{QK} \left(\sum_{s=1}^d c_{T,s} \boldsymbol{\beta}_s \right) \left(\sum_{t=1}^d c_{a,t} \boldsymbol{\beta}_t \right) \left(\sum_{t'=1}^d c_{T,t'} \boldsymbol{\beta}_{t'}^\top \right) \right] \\ &= \frac{1}{d} \sum_{i,j,a,b \in [T]} \mathbb{E} \left[\tilde{\gamma}_a^i \tilde{\gamma}_b^j P_{ij} \sum_{r,s} c_{b,r} c_{T,s} (\boldsymbol{\beta}_r^\top \mathbf{W}_{QK} \boldsymbol{\beta}_s) \sum_{t=1}^d c_{a,t} c_{T,t} \boldsymbol{\beta}_t \boldsymbol{\beta}_t^\top \right] \end{aligned}$$

Due to Semantic Basis Composition assumption, the above expression can be derived:

$$\begin{aligned} \nabla_{\mathbf{W}_{QK}} \mathcal{J} &= \frac{1}{d} \sum_{i,j,a,b \in [T]} \mathbb{E} \left[\tilde{\gamma}_a^i \tilde{\gamma}_b^j P_{ij} \sum_{r,s} c_{b,r} c_{T,s} (\boldsymbol{\beta}_r^\top \mathbf{W}_{QK} \boldsymbol{\beta}_s) \sum_{t=1}^d c_{a,t} c_{T,t} \boldsymbol{\beta}_t \boldsymbol{\beta}_t^\top \right] \\ &= \frac{1}{d} \sum_{i,j,a,b \in [T]} \mathbb{E} \left[\tilde{\gamma}_a^i \tilde{\gamma}_b^j P_{ij} \sum_{r,s} \mu_r \mu_s (\boldsymbol{\beta}_r^\top \mathbf{W}_{QK} \boldsymbol{\beta}_s) \sum_{t=1}^d \mu_t^2 \boldsymbol{\beta}_t \boldsymbol{\beta}_t^\top \right] \\ &= P \left[\sum_{r,s} \mu_r \mu_s (\boldsymbol{\beta}_r^\top \mathbf{W}_{QK} \boldsymbol{\beta}_s) \right] \sum_{t=1}^d \mu_t^2 \boldsymbol{\beta}_t \boldsymbol{\beta}_t^\top, \end{aligned}$$

where, $P = \frac{1}{d} \sum_{i,j,a,b \in [T]} \mathbb{E} \left[\tilde{\gamma}_a^i \tilde{\gamma}_b^j P_{ij} \right]$.

Since $\mathbf{W}_{QK} := \mathbf{W}_Q^\top \mathbf{W}_K$ and the query-key parameters are optimized jointly, we can perform an eigenvalue decomposition on the matrix \mathbf{W}_{QK} , such that $\mathbf{W}_{QK} = \sum_k \sigma_k^2 \mathbf{v}_k \mathbf{v}_k^\top$. By substituting into the expression for $\nabla_{\mathbf{W}_{QK}} \mathcal{J}$, we obtain:

$$\nabla_{\mathbf{W}_{QK}} \mathcal{J} = P \left[\sum_{k=1}^d \sigma_k^2 \sum_{r,s=1}^d \mu_r \mu_s (\boldsymbol{\beta}_r^\top \mathbf{v}_k) (\mathbf{v}_k^\top \boldsymbol{\beta}_s) \sum_{t=1}^d \mu_t^2 \boldsymbol{\beta}_t \boldsymbol{\beta}_t^\top \right]. \quad (13)$$

$\sum_{k=1}^d \sigma_k^2 \sum_{r,s=1}^d \mu_r \mu_s (\beta_r^\top \mathbf{v}_k) (\mathbf{v}_k^\top \beta_s)$ is a scalar.

we decompose:

$$\sum_{k=1}^d \sigma_k^2 \sum_{r,s=1}^d \mu_r \mu_s (\beta_r^\top \mathbf{v}_k) (\mathbf{v}_k^\top \beta_s) = \sigma_1^2 \mu_1^2 (\mathbf{v}_1^\top \beta_1)^2 + 2\sigma_1^2 \sum_{r=2}^d \mu_1 \mu_r (\beta_1^\top \mathbf{v}_1) (\mathbf{v}_1^\top \beta_r) + \sigma_1^2 \sum_{r,s=2}^d \mu_r \mu_s (\beta_r^\top \mathbf{v}_1) (\mathbf{v}_1^\top \beta_s) + \sum_{k=2}^d \sigma_k^2 \sum_{r,s=1}^d \mu_r \mu_s (\beta_r^\top \mathbf{v}_k) (\mathbf{v}_k^\top \beta_s).$$

Due to the representation space naturally exhibits a low stable rank and the Strong Singularity Alignment Assumption, this is bounded as: $\leq \sigma_1^2 \mu_1^2 \left[(1 - \epsilon) + 2 \frac{\epsilon}{d-1} \frac{1}{\text{SR}(\mathbf{Z})} + \frac{\epsilon}{d-1} \frac{1}{\text{SR}(\mathbf{Z})^2} (SR(\mathbf{W}) - 1) \right]$.

The first term, $(1 - \epsilon)$, dominates as μ_1 -dominance and for large d (e.g., 768 in BERT-base), which suppresses subsequent terms. The exact value of ϵ minimally affects the magnitude of subsequent terms, preserving the dominance of $1 - \epsilon$. Thus, we approximate the expression as $\mathcal{O}(\sigma_1^2 \mu_1^2 \phi^2)$.

So we have:

$$\sum_{k=1}^d \sigma_k^2 \sum_{r,s=1}^d \mu_r \mu_s (\beta_r^\top \mathbf{v}_k) (\mathbf{v}_k^\top \beta_s) = \mathcal{O}(\sigma_1^2 \mu_1^2 (\mathbf{v}_1^\top \beta_1)^2)$$

So the gradient expression can be further simplified as follows:

$$\nabla_{\mathbf{W}_{QK}} \mathcal{J} \approx P \mathcal{O}(\sigma_1^2 \mu_1^2 \phi^2) \sum_{t=1} \mu_t^2 \beta_t \beta_t^\top, \quad (14)$$

When \mathbf{W}_{QK} is updated via gradient descent as $\mathbf{W}'_{QK} \leftarrow \mathbf{W}_{QK} - \eta \nabla_{\mathbf{W}_{QK}} \mathcal{J}$, according to matrix perturbation theory, the change in the eigenvalues $\Delta \lambda_l = \Delta \sigma_l^2$ is given by:

$$\Delta \lambda_l = \Delta \sigma_l^2 = \mathbf{v}_l^\top (-\eta \nabla_{\mathbf{W}_{QK}} \mathcal{J}) \mathbf{v}_l.$$

By substituting the form of $\nabla_{\mathbf{W}_{QK}} \mathcal{J}$, the change in the square of each singular value is obtained as:

$$\Delta \sigma_l^2 = -\eta P \mathcal{O}(\sigma_1^2 \mu_1^2 \phi^2) \sum_{t=1} \mu_t^2 (\mathbf{v}_l^\top \beta_t) \quad (15)$$

Therefore, the change in the square of the largest singular value of the parameter matrix is given by:

$$\begin{aligned} \Delta \sigma_1^2 &= -\eta P \mathcal{O}(\sigma_1^2 \mu_1^2 \phi^2) \sum_{t=1} \mu_t^2 (\mathbf{v}_1^\top \beta_t) \\ &= -\eta P \mathcal{O}(\sigma_1^2 \mu_1^4 \phi^4). \end{aligned}$$

Recall the definition of P :

$$P = \frac{1}{d} \sum_{i,j \in [T]} \mathbb{E} \left[\sum_{a,b \in [T]} \tilde{\gamma}_a^i \tilde{\gamma}_b^j \right] P_{ij}.$$

We derive P 's sign by analyzing the expectation, splitting into two cases based on the independence of $\tilde{\gamma}^i$ and $\tilde{\gamma}^j$: (1) $i = j$, and (2) $i \neq j$.

Case 1 ($i = j$): (Coordinate Dependence) When $i = j$, $\tilde{\gamma}^i = \tilde{\gamma}^j$, introducing dependence among coordinates in the truncated $\tilde{\gamma}^i$. If no truncation occurs at index i ($\tilde{\gamma}_i^i \neq 0$), it implies no truncation at any $a \neq i$ ($\tilde{\gamma}_a^i \neq 0$). Define the non-truncation events:

$$E_i = \left\{ \left| \frac{T-1}{T^2} \omega_i + \frac{1}{T^2} \right| \leq c \right\}, \quad E_a = \left\{ \left| \frac{-1}{T^2} \omega_a + \frac{1}{T^2} \right| \leq c \right\}.$$

For large T , the difference between these terms shrinks relative to c , causing $\Pr(E_i)$ to approach $\Pr(E_a)$, resulting in $\Pr(E_a)^2 < \Pr(E_i)$.

We exclude truncation cases yielding zero and focus on non-truncation events. The double sum over $a, b \in [T]$ splits into four subcases:

Subcase 1: $a = b = i$

$$\tilde{\gamma}_i^i \tilde{\gamma}_i^i = \Pr(E_i) \cdot \frac{(T-1)^2}{T^4}.$$

Subcase 2 and 3: $a = i, b \neq i$ or $a \neq i, b = i$ Each term:

$$\tilde{\gamma}_i^i \tilde{\gamma}_b^i = \frac{T-1}{T^2} \cdot \left(-\frac{1}{T^2}\right) = -\frac{T-1}{T^4}.$$

With $2(T-1)$ terms, their expectation is:

$$2(T-1) \cdot \Pr(E_i) \cdot \left(-\frac{T-1}{T^4}\right) = -2 \cdot \Pr(E_i) \cdot \frac{(T-1)^2}{T^4}.$$

Subcase 4: $a \neq i, b \neq i$ Each term:

$$\left(-\frac{1}{T^2}\right)^2 = \frac{1}{T^4},$$

with $(T-1)^2$ terms, yielding:

$$\Pr(E_a)^2 \cdot (T-1)^2 \cdot \frac{1}{T^4}.$$

Combining all subcases:

$$\sum_{a,b} \mathbb{E}[\tilde{\gamma}_a^i \tilde{\gamma}_b^i] = (\Pr(E_a)^2 - \Pr(E_i)) \cdot \frac{(T-1)^2}{T^4}.$$

Thus, the contribution to P for $i = j$ is:

$$\frac{1}{d} \sum_{i=1}^T \mathbb{E} \left[\sum_{a,b \in [T]} \tilde{\gamma}_a^i \tilde{\gamma}_b^i \right] P_{ii} = (\Pr(E_a)^2 - \Pr(E_i)) \cdot \frac{(T-1)^2}{T^4} \cdot \frac{1}{d} \sum_{i=1}^T P_{ii}.$$

Assuming each x_i follows a zero-mean Gaussian,

$$P_{ii} = x_i^\top W_V^\top W_F^\top W_F W_V x_i > 0,$$

since $W_V^\top W_F^\top W_F W_V$ is positive definite and $x_i \neq 0$ almost surely.

Given $\Pr(E_a)^2 < \Pr(E_i)$ (shown earlier), this term is negative:

$$\frac{1}{d} \sum_{i=j} \mathbb{E} \left[\sum_{a,b \in [T]} \tilde{\gamma}_a^i \tilde{\gamma}_b^j \right] P_{ij} < 0.$$

Case 2: $i \neq j$ In this case, we compute the expectation $\mathbb{E}[P_{ij}]$:

$$\mathbb{E}[P_{ij}] = \mathbb{E}[x_i^\top W_V^\top W_F^\top W_F W_V x_j] = \mathbb{E}[\text{Tr}(x_i^\top W_V^\top W_F^\top W_F W_V x_j)] = \text{Tr}(W_V^\top W_F^\top W_F W_V \mathbb{E}[x_j x_i^\top]).$$

Since x_i and x_j are independent, their joint expectation factors as:

$$\mathbb{E}[x_j x_i^\top] = \mathbb{E}[x_j] \mathbb{E}[x_i^\top].$$

For zero-mean inputs, this becomes:

$$\mathbb{E}[x_j x_i^\top] = 0 \Rightarrow \mathbb{E}[P_{ij}] = 0.$$

Thus, in the double sum for $i \neq j$:

$$\frac{1}{d} \sum_{i \neq j} \mathbb{E} \left[\sum_{a,b \in [T]} \tilde{\gamma}_a^i \tilde{\gamma}_b^j \right] P_{ij},$$

all terms vanish, as they depend linearly on $\mathbb{E}[x_i^\top P x_j] = 0$ under independence and zero-mean conditions. Only diagonal terms ($i = j$) contribute to the approximate gradient, with the $i \neq j$ contribution exactly zero.

Combining Case 1 and Case 2 yields $P < 0$, confirming its negativity.

Next, we derive the change in the stable rank of the parameter matrix \mathbf{W}_K . We further assume that \mathbf{v}_l ($l \neq 1$) is not aligned with any of the non-dominant features, meaning it has the same angle with each of them. Thus, $\mathbf{v}_l^\top \boldsymbol{\beta}_i = \frac{1}{\sqrt{d-1}}$.

Therefore, due to Equation 15, we have:

$$\begin{aligned}\Delta\sigma_1^2 &\approx -\eta P \mathcal{O}(\sigma_1^2 \mu_1^2 \phi^2) \mu_1^2 \phi^2 \\ \Delta\sigma_l^2 &= -\eta P \mathcal{O}(\sigma_1^2 \mu_1^2 \phi^2) \sum_{t=2}^d \mu_t^2 (\mathbf{v}_l^\top \boldsymbol{\beta}_t)^2 \\ &= -\eta P \mathcal{O}(\sigma_1^2 \mu_1^2 \phi^2) \frac{1}{d-1} \sum_{t=2}^d \mu_t^2 \\ &= -\eta P \mathcal{O}(\sigma_1^2 \mu_1^2 \phi^2) \frac{\mu_1^2}{d-1} (\text{SR}(\mathbf{Z}) - 1)\end{aligned}$$

We define $\text{SR}(\mathbf{W}) = \frac{A}{B}$, where $A = \sum_{i=1}^d \sigma_i^2$ and $B = \sigma_1^2$. After the update, $\text{SR}(\mathbf{W}') = \frac{A+\delta A}{B+\delta B}$, where $\delta A = -\eta P \mathcal{O}(\sigma_1^2 \mu_1^2 \phi^2) \mu_1^2 [\phi^2 + \text{SR}(\mathbf{Z}) - 1]$ and $\delta B = -\eta P \mathcal{O}(\sigma_1^2 \mu_1^2 \phi^2) \mu_1^2 \phi^2$.

Thus we have

$$\begin{aligned}\Delta \text{SR}(\mathbf{W}) &= \text{SR}(\mathbf{W}') - \text{SR}(\mathbf{W}) \\ &= \frac{A+\delta A}{B+\delta B} - \frac{A}{B} \\ &= (A+\delta A) \left(\frac{1}{B} - \frac{\delta B}{B^2} \right) \\ &\approx \frac{\delta A}{B} - \frac{A\delta B}{B^2} \\ &= -\eta P \mathcal{O}(\mu_1^2 \phi^2) \mu_1^2 \mathbf{R},\end{aligned}$$

where $\mathbf{R} = [(1 - \text{SR}(\mathbf{W}_K)) \phi^2 + (\text{SR}(\mathbf{Z}) - 1)]$.

So when the following condition is satisfied:

$$\text{SR}(\mathbf{W}_K) > 1 + \frac{\text{SR}(\mathbf{Z}) - 1}{\phi^2}, \quad (16)$$

the $\text{SR}(\mathbf{W}_K)$ will decrease with the update. □

A.2 Amplification of Singularity Alignment.

Theorem A.2 (Amplification of Singularity Alignment). *Let \mathbf{W}_{QK} be updated using the gradient $\nabla_{\mathbf{W}_{QK}} \mathcal{J}$ as in Equation 5. The singular alignment ϕ between \mathbf{W}_{QK} and \mathbf{Z} increases after the update. The change in alignment is given by:*

$$\Delta\phi = -\eta P \mathcal{O}(\sigma_1^2 \mu_1^2 \phi^2) \mu_1^2 \phi \sum_{k \neq 1} \frac{(\mathbf{v}_k^\top \boldsymbol{\beta}_1)^2}{\sigma_1^2 - \sigma_k^2}, \quad (17)$$

indicating a positive update of ϕ .

Proof. \mathbf{W}_{QK} is updated with $(\Delta \mathbf{W}_{QK}) = -\eta \nabla_{\mathbf{W}_{QK}} \mathcal{J}$. When the matrix perturbation is sufficiently small, according to Rayleigh–Schrödinger perturbation theory, the change in the new singular vector of \mathbf{W}_K is given by:

$$\mathbf{v}'_i = \mathbf{v}_i + \sum_{k \neq i} \frac{\mathbf{v}_k^\top (\Delta \mathbf{W}_{QK}) \mathbf{v}_i}{\sigma_i^2 - \sigma_k^2} \mathbf{v}_k + O(\|\Delta \mathbf{W}_{QK}\|^2)$$

So we have:

$$\begin{aligned}\mathbf{v}'_1 &= \mathbf{v}_1 + \sum_{k \neq 1} \frac{\mathbf{v}_k^\top (\Delta \mathbf{W}_{QK}) \mathbf{v}_1}{\sigma_1^2 - \sigma_k^2} \mathbf{v}_k + \mathcal{O}(\|\Delta \mathbf{W}_{QK}\|^2) \\ &= \mathbf{v}_1 + (-\eta P \mathcal{O}(\sigma_1^2 \mu_1^2 \phi^2)) \sum_{k \neq 1} \frac{\mathbf{v}_k^\top (\sum_{t=1}^d \mu_t^2 \beta_t \beta_t^\top) \mathbf{v}_1}{\sigma_1^2 - \sigma_k^2} \mathbf{v}_k + \mathcal{O}(\|\Delta \mathbf{W}_{QK}\|^2)\end{aligned}$$

So the new singularity alignment ϕ' is:

$$\begin{aligned}\phi' &= \beta_1^\top \mathbf{v}'_1 = \beta_1^\top \mathbf{v}_1 + (-\eta P \mathcal{O}(\sigma_1^2 \mu_1^2 \phi^2)) \sum_{k \neq 1} \frac{\mathbf{v}_k^\top (\sum_{t=1}^d \mu_t^2 \beta_t \beta_t^\top) \mathbf{v}_1}{\sigma_1^2 - \sigma_k^2} \beta_1^\top \mathbf{v}_k + \mathcal{O}(\|\Delta \mathbf{W}_{QK}\|^2) \\ &= \beta_1^\top \mathbf{v}_1 + (-\eta P \mathcal{O}(\sigma_1^2 \mu_1^2 \phi^2)) \sum_{t=1}^d \mu_t^2 \sum_{k \neq 1} \frac{(\mathbf{v}_k^\top \beta_t)(\beta_t^\top \mathbf{v}_1)}{\sigma_1^2 - \sigma_k^2} \beta_1^\top \mathbf{v}_k + \mathcal{O}(\|\Delta \mathbf{W}_{QK}\|^2)\end{aligned}$$

Due to the Strong Singularity Alignment assumption, we have:

$$\phi' = \beta_1^\top \mathbf{v}_1 + (-\eta P \mathcal{O}(\sigma_1^2 \mu_1^2 \phi^2)) \left[\mu_1^2 \phi \sum_{k \neq 1} \frac{(\mathbf{v}_k^\top \beta_1)^2}{\sigma_1^2 - \sigma_k^2} + \mathcal{O}(\epsilon) \right] + \mathcal{O}(\|\Delta \mathbf{W}_{QK}\|^2)$$

Ignoring $\mathcal{O}(\epsilon)$ and $\mathcal{O}(\|\Delta \mathbf{W}_{QK}\|^2)$, we obtain:

$$\Delta \phi \approx -\eta P \sigma_1^2 \mathcal{O}(\mu_1^2 \phi^2) \mu_1^2 \phi \sum_{k \neq 1} \frac{(\mathbf{v}_k^\top \beta_1)^2}{\sigma_1^2 - \sigma_k^2}$$

□

A.3 Amplification of Representation Singularity

Theorem A.3 (Amplification of Representation Singularity). *We study the Key-Query inner product in a one-layer Transformer: $\mathbf{Z}_K^\top \mathbf{Z}_Q = \mathbf{Z} \mathbf{W}_{QK} \mathbf{Z}^\top$, then the stable rank of \mathbf{Z}_K and \mathbf{Z}_Q is:*

$$\text{SR}(\mathbf{Z}_K) = \text{SR}(\mathbf{Z}_Q) \approx 1 + \frac{[\text{SR}(\mathbf{W}_K) - 1][\text{SR}(\mathbf{Z}) - 1]}{(d-1)\phi^2} \quad (18)$$

Let \mathbf{W}_{QK} be updated using the simplified gradient $\nabla_{\mathbf{W}_{QK}} \mathcal{J}$ as in Equation 5. Then if the following condition being satisfied: $\text{SR}(\mathbf{W}_K) > 1 + \frac{\phi^2 [\text{SR}(\mathbf{Z}) - 1]}{(d-1)^2}$, $\text{SR}(\mathbf{Z}_K)$ decreases.

Proof. We first derive the form of the Key-Query inner product $\mathbf{Z}_K^\top \mathbf{Z}_Q$, thereby obtaining the singular vectors and singular values.

$$\begin{aligned}\mathbf{Z}_K^\top \mathbf{Z}_Q &= \mathbf{Z} \mathbf{W}_{QK} \mathbf{Z}^\top \\ &= (\sum_{i=1}^d \mu_i \boldsymbol{\alpha}_i \boldsymbol{\beta}_i^\top) (\sum_{t=1}^d \sigma_t^2 \mathbf{v}_t \mathbf{v}_t^\top) (\sum_{j=1}^d \mu_j \boldsymbol{\beta}_j \boldsymbol{\alpha}_j^\top) \\ &= \sum_{t=1}^d \sigma_t^2 \sum_{i,j} \mu_i \mu_j (\boldsymbol{\alpha}_i \boldsymbol{\beta}_i^\top \mathbf{v}_t \mathbf{v}_t^\top \boldsymbol{\beta}_j \boldsymbol{\alpha}_j^\top) \\ &= \sigma_1^2 \sum_{i,j} (\boldsymbol{\alpha}_i \boldsymbol{\beta}_i^\top \mathbf{v}_1 \mathbf{v}_1^\top \boldsymbol{\beta}_j \boldsymbol{\alpha}_j^\top) + \sum_{t=2}^d \sigma_t^2 \sum_{i,j} \mu_i \mu_j (\boldsymbol{\alpha}_i \boldsymbol{\beta}_i^\top \mathbf{v}_t \mathbf{v}_t^\top \boldsymbol{\beta}_j \boldsymbol{\alpha}_j^\top)\end{aligned}$$

We further assume that \mathbf{v}_l ($l \neq 1$) is not aligned with any of the non-dominant features, meaning it has the same angle with each of them. Thus, $\mathbf{v}_l^\top \boldsymbol{\beta}_i = \frac{1}{\sqrt{d-1}}$. And due to Strong Singularity Alignment Assumption, we have:

$$\begin{aligned}\mathbf{Z}_K^\top \mathbf{Z}_Q &= \sigma_1^2 \mu_1^2 \phi^2 \boldsymbol{\alpha}_1 \boldsymbol{\alpha}_1^\top + (\sum_{t=2}^d \sigma_t^2) \frac{1}{d-1} \sum_{i,j} \mu_i \mu_j \boldsymbol{\alpha}_i \boldsymbol{\alpha}_j^\top + \mathcal{O}(\epsilon) + \mathcal{O}(\epsilon^2) \\ &= \sigma_1^2 \mu_1^2 \phi^2 \boldsymbol{\alpha}_1 \boldsymbol{\alpha}_1^\top + (\text{SR}(\mathbf{W}_K) - 1) \sigma_1^2 \frac{1}{d-1} \sum_{i,j} \mu_i \mu_j \boldsymbol{\alpha}_i \boldsymbol{\alpha}_j^\top + \mathcal{O}(\epsilon) + \mathcal{O}(\epsilon^2)\end{aligned}$$

So we get the approximated singular value and singular vectors of \mathbf{Z}_K and \mathbf{Z}_Q :

$$\sigma_1^2(\mathbf{Z}_K) \approx \sigma_1^2 \mu_1^2 \phi^2,$$

with corresponding singular vector: $\mathbf{v}_1(\mathbf{Z}_K) = \boldsymbol{\alpha}_1$, and

$$\sigma_2^2(\mathbf{Z}_K) \approx (\text{SR}(\mathbf{W}_K) - 1) \sigma_1^2 \frac{1}{d-1} (\text{SR}(\mathbf{Z}) - 1) \mu_1^2,$$

with corresponding singular vector: $\mathbf{v}_2(\mathbf{Z}_K) = \frac{1}{\sqrt{\sum_{i=2}^d \mu_i^2}} \sum_{i=2}^d \boldsymbol{\alpha}_i$. The remaining singular values and singular vectors are primarily contributed by $\mathcal{O}(\epsilon) + \mathcal{O}(\epsilon^2)$, which can be neglected.

So the Stable rank of \mathbf{Z}_K and \mathbf{Z}_Q can be approximated as:

$$\begin{aligned} \text{SR}(\mathbf{Z}_K) &\approx \frac{\sigma_1^2 \mu_1^2 \phi^2 + (\text{SR}(\mathbf{W}_K) - 1) \sigma_1^2 \frac{1}{d-1} (\text{SR}(\mathbf{Z}) - 1) \mu_1^2}{\sigma_1^2 \mu_1^2 \phi^2} \\ &= 1 + \frac{[\text{SR}(\mathbf{W}_K) - 1] [\text{SR}(\mathbf{Z}) - 1]}{(d-1) \phi^2} \end{aligned}$$

Then, we derive the changes in the singular values of $\mathbf{Z}_K^\top \mathbf{Z}_Q$ after the update of W_{QK} .

$$\begin{aligned} \Delta \mathbf{Z}_K^\top \mathbf{Z}_Q &= \mathbf{Z}(-\eta \nabla_{\mathbf{W}_{QK}} \mathcal{J}) \mathbf{Z}^\top \\ &= (-\eta P \mathcal{O}(\sigma_1^2 \mu_1^2 \phi^2)) \left(\sum_{i=1}^d \mu_i \boldsymbol{\alpha}_i \boldsymbol{\beta}_i^\top \right) \left(\sum_{t=1}^d \mu_t^2 \boldsymbol{\beta}_t \boldsymbol{\beta}_t^\top \right) \left(\sum_{j=1}^d \mu_j \boldsymbol{\beta}_j \boldsymbol{\alpha}_j^\top \right) \\ &= (-\eta P \mathcal{O}(\sigma_1^2 \mu_1^2 \phi^2)) \sum_{t=1}^d \mu_t^2 \sum_{i,j} \mu_i \mu_j (\boldsymbol{\alpha}_i \boldsymbol{\beta}_i^\top \boldsymbol{\beta}_t \boldsymbol{\beta}_t^\top \boldsymbol{\beta}_i \boldsymbol{\alpha}_j^\top) \\ &= (-\eta P \mathcal{O}(\sigma_1^2 \mu_1^2 \phi^2)) \sum_{t=1}^d \mu_t^4 \boldsymbol{\alpha}_t \boldsymbol{\alpha}_t^\top \end{aligned}$$

So the change of the square of singular values of $\mathbf{Z}_K^\top \mathbf{Z}_Q$ is:

$$\begin{aligned} \Delta \sigma_1^2(\mathbf{Z}_K) &= \mathbf{v}_1^\top(\mathbf{Z}_K) \Delta \mathbf{Z}_K^\top \mathbf{Z}_Q \mathbf{v}_1(\mathbf{Z}_K) \\ &= (-\eta P \mathcal{O}(\sigma_1^2 \mu_1^2 \phi^2)) \boldsymbol{\alpha}_1^\top \sum_{t=1}^d \mu_t^4 \boldsymbol{\alpha}_t \boldsymbol{\alpha}_t^\top \boldsymbol{\alpha}_1 \\ &= (-\eta P \mathcal{O}(\sigma_1^2 \mu_1^2 \phi^2)) \mu_1^4 \end{aligned}$$

$$\begin{aligned} \Delta \sigma_2^2(\mathbf{Z}_K) &= \mathbf{v}_2^\top(\mathbf{Z}_K) \Delta \mathbf{Z}_K^\top \mathbf{Z}_Q \mathbf{v}_2(\mathbf{Z}_K) \\ &= (\eta P \mathcal{O}(\sigma_1^2 \mu_1^2 \phi^2)) \left(\frac{1}{\sqrt{\sum_{t=2}^d \mu_t^2}} \sum_{i=2}^d \boldsymbol{\alpha}_i \right)^\top \left(\sum_{t=1}^d \mu_t^4 \boldsymbol{\alpha}_t \boldsymbol{\alpha}_t^\top \right) \left(\frac{1}{\sqrt{\sum_{t=2}^d \mu_t^2}} \sum_{i=2}^d \boldsymbol{\alpha}_i \right) \\ &= (\eta P \mathcal{O}(\sigma_1^2 \mu_1^2 \phi^2)) \frac{\sum_{i=2}^d \mu_i^6}{(\text{SR}(\mathbf{Z}) - 1) \mu_1^2} \\ &\approx (\eta P \mathcal{O}(\sigma_1^2 \mu_1^2 \phi^2)) \frac{(\text{SR}(\mathbf{Z}) - 1)^2 \mu_1^4}{(d-1)^3} \end{aligned}$$

So if $\frac{\Delta \sigma_1^2(\mathbf{Z}_K) + \Delta \sigma_2^2(\mathbf{Z}_K)}{\Delta \sigma_1^2(\mathbf{Z}_K)} < \text{SR}(\mathbf{Z}_K)$, which is that

$$\text{SR}(\mathbf{W}_K) > 1 + \frac{\phi^2 [\text{SR}(\mathbf{Z}) - 1]}{(d-1)^2},$$

$\text{SR}(\mathbf{Z}_K)$ decreases.

□

A.4 Lower and Upper bound of gradient's Frobenius norm

Theorem A.4 (Bounds on Gradient Frobenius Norm). *The Frobenius norm of the QK -gradient $\nabla_{\mathbf{W}_{QK}} \mathcal{J}$ is bounded as follows:*

1. *Lower Bound: Assuming a fixed Frobenius norm $\|\mathbf{W}_{QK}\|_F^2 = \sum_{k=1}^d \sigma_k^2 = M > 0$ at a given step, the gradient norm satisfies:*

$$\|\nabla_{\mathbf{W}_{QK}} \mathcal{J}\|_F \geq K \alpha_1 \sigma_1^2(\mathbf{W}_{QK}), \quad (19)$$

where $K = P \cdot \|\sum_{t=1}^d \mu_t^2 \boldsymbol{\beta}_t \boldsymbol{\beta}_t^\top\| > 0$ and $\alpha_1 = \left(\sum_{r=1}^d \mu_r \cdot (\mathbf{v}_1^\top \boldsymbol{\beta}_r) \right)^2$.

2. *Upper Bound:*

$$\|\nabla_{\mathbf{W}_{QK}} \mathcal{J}\|_F \leq C \sigma_1^2(\mathbf{W}_V) [\sigma_1(\mathbf{W}_{F_1}) \sigma_1(\mathbf{W}_{F_2}) + 1]^2 \sigma_1(\mathbf{W}_{QK}), \quad (20)$$

where $C = \frac{1}{d} \sum_{i,j,a,b \in [T]} \mathbb{E} \left[\tilde{\gamma}_a^i \tilde{\gamma}_b^j \right] \mathcal{O}(\mu_1^4 \phi^2) \text{SR}(\mathbf{Z})$.

Proof. In the simplified single layer transformer, The gradient of \mathbf{W}_{QK} can be approximated as:

$$\nabla_{\mathbf{W}_{QK}} \mathcal{J} \approx P \mathcal{O}(\sigma_1^2 \mu_1^2 \phi^2) \sum_{t=1}^d \mu_t^2 \boldsymbol{\beta}_t \boldsymbol{\beta}_t^\top,$$

where $P = \frac{1}{d} \sum_{i,j,a,b \in [T]} \mathbb{E} \left[\tilde{\gamma}_a^i \tilde{\gamma}_b^j P_{ij} \right]$.

We first bound P :

$$\begin{aligned} P &= \frac{1}{d} \sum_{i,j,a,b \in [T]} \mathbb{E} \left[\tilde{\gamma}_a^i \tilde{\gamma}_b^j P_{ij} \right] \\ &= \frac{1}{d} \sum_{i,j,a,b \in [T]} \mathbb{E} \left[\tilde{\gamma}_a^i \tilde{\gamma}_b^j \mathbf{x}_i^\top \mathbf{W}_V^\top \mathbf{W}_F^\top \mathbf{W}_F \mathbf{W}_V \mathbf{x}_j \right] \\ &\leq \frac{1}{d} \sum_{i,j,a,b \in [T]} \mathbb{E} \left[\tilde{\gamma}_a^i \tilde{\gamma}_b^j \right] \sigma_1^2(\mathbf{W}_V) [\sigma_1(\mathbf{W}_{F_1}) \sigma_1(\mathbf{W}_{F_2}) + 1]^2 \end{aligned}$$

Then we bound $\sum_{t=1}^d \mu_t^2 \boldsymbol{\beta}_t \boldsymbol{\beta}_t^\top$:

$$\begin{aligned} \left\| \sum_{t=1}^d \mu_t^2 \boldsymbol{\beta}_t \boldsymbol{\beta}_t^\top \right\|_F &\leq \sum_{t=1}^d \mu_t^2 \|\boldsymbol{\beta}_t\|^2 \\ &\leq \sum_{t=1}^d \mu_t^2 \end{aligned}$$

Thus the F-Norm of QK -gradient $\nabla_{\mathbf{W}_{QK}} J$ is upper bounded by:

$$\|\nabla_{\mathbf{W}_{QK}} J\|_F \leq C \sigma_1^2(\mathbf{W}_V) [\sigma_1(\mathbf{W}_{F_1}) \sigma_1(\mathbf{W}_{F_2}) + 1]^2 \sigma_1(\mathbf{W}_{QK}),$$

where $C = \frac{1}{d} \sum_{i,j,a,b \in [T]} \mathbb{E} \left[\tilde{\gamma}_a^i \tilde{\gamma}_b^j \right] \mathcal{O}(\mu_1^4 \phi^2) \text{SR}(\mathbf{Z})$.

Through equation 13, the gradient can be approximated as

$$\nabla_{\mathbf{W}_{QK}} \mathcal{J} = P \left[\sum_{k=1}^d \sigma_k^2 \sum_{r,s=1}^d \mu_r \mu_s (\boldsymbol{\beta}_r^\top \mathbf{v}_k) (\mathbf{v}_k^\top \boldsymbol{\beta}_s) \sum_{t=1}^d \mu_t^2 \boldsymbol{\beta}_t \boldsymbol{\beta}_t^\top \right]. \quad (21)$$

Rearranging terms and defining

$$\alpha_k := \left(\sum_{r=1}^d \mu_r \mathbf{v}_k^\top \boldsymbol{\beta}_r \right)^2 = (\mathbf{v}_k^\top \mathbf{p})^2, \quad \text{where } \mathbf{p} := \sum_{r=1}^d \mu_r \boldsymbol{\beta}_r,$$

we rewrite the gradient as

$$\nabla_{\mathbf{W}_{QK}} \mathcal{J} = P \left[\sum_{k=1}^d \sigma_k^2 \alpha_k \cdot \sum_{t=1}^d \mu_t^2 \beta_t \beta_t^\top \right].$$

Gradient norm depends only on $\sum_k \sigma_k^2 \alpha_k$: Observe that both P and $\sum_{t=1}^d \mu_t^2 \beta_t \beta_t^\top$ are independent of the matrix \mathbf{W}_{QK} 's singular values $\{\sigma_k^2\}$. Therefore, the gradient magnitude (under Frobenius or spectral norm) depends linearly on the scalar quantity

$$\sum_{k=1}^d \sigma_k^2 \alpha_k.$$

Lower bound on α_1 .

By definition:

$$\mathbf{v}_1^\top \mathbf{p} = \sum_{r=1}^d \mu_r (\mathbf{v}_1^\top \beta_r) = \mu_1 (\mathbf{v}_1^\top \beta_1) + \sum_{r=2}^d \mu_r (\mathbf{v}_1^\top \beta_r).$$

Using Assumption: $-\mathbf{v}_1^\top \beta_1 = \sqrt{1-\epsilon}$, - and for $r \geq 2$, $|\mathbf{v}_1^\top \beta_r| \leq \sqrt{\epsilon}$, - also, $\mu_r \leq \mu_1$ for all r , and $\sum_{r=2}^d \mu_r \leq \frac{1}{\eta} \mu_1 - \mu_1 \leq \left(\frac{1}{\eta} - 1\right) \mu_1$.

Therefore:

$$|\sum_{r=2}^d \mu_r (\mathbf{v}_1^\top \beta_r)| \leq \left(\sum_{r=2}^d \mu_r \right) \cdot \sqrt{\epsilon} \leq \left(\frac{1}{\eta} - 1 \right) \mu_1 \sqrt{\epsilon}.$$

Hence:

$$\mathbf{v}_1^\top \mathbf{p} \geq \mu_1 \sqrt{1-\epsilon} - \left(\frac{1}{\eta} - 1 \right) \mu_1 \sqrt{\epsilon} = \mu_1 \left(\sqrt{1-\epsilon} - \left(\frac{1}{\eta} - 1 \right) \sqrt{\epsilon} \right).$$

Let us denote:

$$L := \mu_1 \left(\sqrt{1-\epsilon} - \left(\frac{1}{\eta} - 1 \right) \sqrt{\epsilon} \right).$$

Then,

$$\alpha_1 = (\mathbf{v}_1^\top \mathbf{p})^2 \geq L^2.$$

Upper bound on α_k for $k > 1$

Similarly, for $k > 1$, we write:

$$\alpha_k = (\mathbf{v}_k^\top \mathbf{p})^2 = \left(\sum_{r=1}^d \mu_r (\mathbf{v}_k^\top \beta_r) \right)^2.$$

From the orthonormality of $\{\mathbf{v}_k\}$ and $\{\beta_r\}$, we have:

$$\sum_{k=1}^d (\mathbf{v}_k^\top \beta_1)^2 = 1.$$

Since $\mathbf{v}_1^\top \beta_1 = \sqrt{1-\epsilon}$, we get:

$$\sum_{k>1} (\mathbf{v}_k^\top \beta_1)^2 \leq \epsilon, \quad \Rightarrow \quad \max_{k>1} |\mathbf{v}_k^\top \beta_1| \leq \sqrt{\epsilon}.$$

Also, $|\mathbf{v}_k^\top \beta_r| \leq 1$ for all r . So we can bound:

$$|\mathbf{v}_k^\top \mathbf{p}| = \left| \sum_{r=1}^d \mu_r (\mathbf{v}_k^\top \beta_r) \right| \leq \mu_1 \left(\sqrt{\epsilon} + \left(\frac{1}{\eta} - 1 \right) \right).$$

Define:

$$U := \mu_1 \left(\sqrt{\epsilon} + \left(\frac{1}{\eta} - 1 \right) \right), \quad \Rightarrow \quad \alpha_k \leq U^2.$$

We now compare the bounds:

$$\alpha_1 \geq L^2, \quad \alpha_k \leq U^2 \quad (k > 1).$$

Thus, to ensure $\alpha_1 > \alpha_k$ for all $k > 1$, it suffices that

$$L^2 > U^2, \quad \text{or equivalently} \quad \sqrt{1-\epsilon} - \left(\frac{1}{\eta} - 1 \right) \sqrt{\epsilon} > \sqrt{\epsilon} + \left(\frac{1}{\eta} - 1 \right).$$

This inequality clearly holds when: $\epsilon \ll 1$, $\eta \approx 1$ (i.e., μ_1 is strongly dominant), and d is moderate.

Then we will prove Gradient norm increases when more energy is concentrated on σ_1 .

Now, define:

$$S := \sum_{k=1}^d \sigma_k^2 \alpha_k.$$

We will now prove that S increases as σ_1^2 increases, i.e., when more energy is concentrated on the top singular value.

Let $\sigma^2 := (\sigma_1^2, \dots, \sigma_d^2)$ be any distribution of energy with $\sum_k \sigma_k^2 = C$

Define an energy transfer operation: for small $\varepsilon > 0$, move energy from σ_j^2 to σ_1^2 , i.e.,

$$\sigma_1^{2'} = \sigma_1^2 + \varepsilon, \quad \sigma_j^{2'} = \sigma_j^2 - \varepsilon, \quad \text{with all other } \sigma_k^2 \text{ unchanged.}$$

This preserves total energy:

$$\sum_{k=1}^d \sigma_k^{2'} = C.$$

Then, the corresponding change in S is:

$$S' - S = \varepsilon(\alpha_1 - \alpha_j).$$

But since $\alpha_1 > \alpha_j$, we have $S' > S$. Hence, moving energy from lower-weighted singular directions to the top singular direction strictly increases the gradient norm.

Maximizer of S under $\sum_k \sigma_k^2 = C$:

Because $\alpha_1 > \alpha_2 \geq \dots \geq \alpha_d$, the linear objective $\sum_k \sigma_k^2 \alpha_k$ is maximized under the constraint $\sum_k \sigma_k^2 = C$ when:

$$\sigma_1^2 = C, \quad \sigma_k^2 = 0 \text{ for } k > 1.$$

Due to $\|\nabla_{\mathbf{W}_{QK}} \mathcal{J}\| = K \cdot \sum_{k=1}^d \sigma_k^2 \alpha_k$, and $\alpha_1 > \alpha_k$ and all $\sigma_k^2 \geq 0$, we have:

$$\sum_{k=1}^d \sigma_k^2 \alpha_k \geq \sigma_1^2 \alpha_1.$$

Thus,

$$\|\nabla_{\mathbf{W}_{QK}} \mathcal{J}\| \geq K \cdot \sum_k \sigma_k^2 \alpha_k \geq K \cdot \alpha_1 \cdot \sigma_1^2.$$

□

B Empirical Validation of Theorem Robustness

The Strong Singularity Alignment assumption—where the top singular vector v_1 of the parameter matrix aligns closely with the dominant semantic basis vector β_1 , i.e., $v_1^\top \beta_1 = \sqrt{1 - \epsilon}$ with $\epsilon \rightarrow 0$ —simplifies our theoretical analysis. It holds when this alignment significantly exceeds other vector pairings, a condition met across practical regimes. While Fig 1 shows alignment near 0.8, not 1, this remains sufficient for our results, as detailed below.

The assumption underpins two key analyses:

1. Gradient Approximation Bounds: Under the given assumptions, we decompose:
$$\sum_{k=1}^d \sigma_k^2 \sum_{r,s=1}^d \mu_r \mu_s (\beta_r^\top \mathbf{v}_k) (\mathbf{v}_k^\top \beta_s) = \sigma_1^2 \mu_1^2 (\mathbf{v}_1^\top \beta_1)^2 + 2\sigma_1^2 \sum_{r=2}^d \mu_1 \mu_r (\beta_1^\top \mathbf{v}_1) (\mathbf{v}_1^\top \beta_r) + \sigma_1^2 \sum_{r,s=2}^d \mu_r \mu_s (\beta_r^\top \mathbf{v}_1) (\mathbf{v}_1^\top \beta_s) + \sum_{k=2}^d \sigma_k^2 \sum_{r,s=1}^d \mu_r \mu_s (\beta_r^\top \mathbf{v}_k) (\mathbf{v}_k^\top \beta_s).$$

This is bounded as: $\leq \sigma_1^2 \mu_1^2 \left[(1 - \epsilon) + 2 \frac{\epsilon}{d-1} \frac{1}{\text{SR}(\mathbf{Z})} + \frac{\epsilon}{d-1} \frac{1}{\text{SR}(\mathbf{Z})^2} + \frac{1}{d} \frac{1}{\text{SR}(\mathbf{Z})^2} (\text{SR}(\mathbf{W}) - 1) \right]$. The first term, $(1 - \epsilon)$, dominates as μ_1 -dominance) and for large d (e.g., 768 in BERT-base), which suppresses subsequent terms. The exact value of ϵ minimally affects the magnitude of subsequent terms, preserving the dominance of $1 - \epsilon$. Thus, we approximate the expression as $\mathcal{O}(\sigma_1^2 \mu_1^2 \phi^2)$, contributing to Equation (3) in Theorem 2.1, with similar bounds like $\mathcal{O}(\mu_1^2 \phi^2)$ derived analogously.

2. σ_1 and $\text{SR}(W_{KQ})$ Dynamics: The shift in squared singular values, $\Delta \sigma_l^2 = -\eta \cdot \mathcal{P} \cdot \mathcal{O}(\sigma_1^2 \mu_1^2 \phi^2) \sum_{t=1}^d \mu_t^2 (\mathbf{v}_l^\top \beta_t)^2$, drives a simultaneous increase in σ_1 and decrease in $\text{SR}(W_{KQ})$ via the dominant term $\mu_1^2 (\mathbf{v}_1^\top \beta_1)^2$. This dominance stems from: (a) μ_1 exceeding other μ_i much, and (b) the singularity alignment $v_1^\top \beta_1 = \sqrt{1 - \epsilon}$ greatly exceeding other pairings $(\mathbf{v}_l^\top \beta_t)^2, l \neq 1, t \neq 1$. In our experiments (hidden dimension 768), $v_1^\top \beta_1 = 0.8$ ($\epsilon = 0.36$, $(\mathbf{v}_1^\top \beta_1)^2 = 0.64$) yields an expected $(\mathbf{v}_l^\top \beta_i)^2$ or $(\mathbf{v}_i^\top \beta_1)^2$ ($i \neq 1$) of 3.8×10^{-4} —three orders smaller—ensuring $\Delta \sigma_1^2$ overshadows $\sum_{l \neq 1} \Delta \sigma_l^2$, sustaining this dynamic.

C Method Details

C.1 Smoothing Policy

Given a weight matrix \mathbf{W} and its dominant singular values $\sigma = \{\sigma_i\}_{i=1}^{\lceil \text{SR}(\mathbf{W}) \rceil}$, we introduce several smoothing functions below.

Convolution. We apply a convolution kernel $\mathbf{k} = \{k_j\}_{j=-m}^m$ to the dominant singular values σ to smooth the transition between them. The smoothed singular values $\sigma^{\text{smooth}} = \{\sigma_i^{\text{smooth}}\}$ are computed by convolving the kernel with the original singular values:

$$\sigma_i^{\text{smooth}} = \sum_{j=-m}^m k_j \cdot \sigma_{i+j}, \quad \forall i \in \{m+1, \dots, \lceil \text{SR}(\mathbf{W}) \rceil - m\}$$

where σ_{i+j} refers to neighboring singular values, and the kernel \mathbf{k} is typically normalized to ensure that the sum of the kernel elements equals 1:

$$\sum_{j=-m}^m k_j = 1.$$

This convolution operation smooths the singular value spectrum by averaging over a local neighborhood of values. It reduces abrupt changes between adjacent singular values while preserving their relative order, ensuring that the most dominant singular values retain their influence in the parametric space.

Softmax. We apply the Softmax function to the dominant singular values $\sigma = \{\sigma_i\}_{i=1}^{\lceil \text{SR}(\mathbf{W}) \rceil}$ to ensure that the singular values are normalized while retaining their relative importance. The Softmax-smoothed singular values $\sigma_i^{\text{softmax}} = \{\sigma_i^{\text{softmax}}\}$ are computed as follows:

$$\sigma_i^{\text{softmax}} = \frac{\exp(\beta \cdot \sigma_i)}{\sum_{j=1}^{\lceil \text{SR}(\mathbf{W}) \rceil} \exp(\beta \cdot \sigma_j)}$$

$$\sigma_i^* = \frac{\exp(\beta \cdot \sigma_i)}{\sum_{j=1}^n \exp(\beta \cdot \sigma_j)}$$

where β is a scaling parameter that controls the sharpness of the distribution. A higher β places more emphasis on the larger singular values, while a lower β spreads the emphasis more evenly across all singular values.

The Softmax function smooths the singular values by normalizing them in a way that maintains the hierarchy of dominance, but it prevents any one singular value from dominating excessively. This ensures that the singular value distribution remains balanced and well-behaved during the smoothing process.

D Experiment details

D.1 Model Configuration Details

The detailed training configuration of BERT and GPT-2 is shown in Table 4 and Table 5.

Table 4: Configuration of BERT training.

Configurations	BERT-base	BERT-large
Hidden activation	GELU	
Max position embeddings	512	
Tokenizer		RoBERTa-base
Vocabulary size	50265	
Sequence length	128	
Layernorm ϵ	1e-12	
Dropout probability	0.1	
Optimizer		AdamW
AdamW weight decay	0.01	
AdamW (β_1, β_2)		(0.9, 0.999)
AdamW ϵ	0.01	
LR warm-up steps	1000	
LR scheduler		Cosine
Hidden size	768	1024
Intermediate size		$4 \times$ Hidden size
Hidden Layers	12	24
Num. attention heads	12	16
Batch size	64	32

Table 5: Configuration of GPT-2 training.

Configurations	GPT-2-medium	GPT-2-large	GPT-2-XL
Hidden activation	GELU		
Max position embeddings	512		
Tokenizer	r50-k		
Vocabulary size	50257		
Sequence length	256		
Layernorm ϵ	1e-5		
Dropout probability	0.5		
Optimizer	AdamW		
AdamW weight decay	0.1		
AdamW (β_1, β_2)	(0.9, 0.995)		
AdamW ϵ	0.01		
LR warm-up steps	1000		
LR scheduler	Linear		
Hidden size	1024	1280	1600
Intermediate size		4 \times Hidden size	
Hidden Layers	24	36	48
Num. attention heads	16	20	25
Batch size	64	32	16

D.2 Loss Curve with Different Stabilization Methods

Fig. 4 illustrates the test loss curves on BERT-base at LRs of 1e-4 and 4e-4. PSS detects and stabilizes loss explosions with minimal spikes and no additional training steps to recover. In contrast, GC and OR fail to prevent instability and result in training failure. QK-Norm, while stabilizing training, does so at the cost of increased test loss.

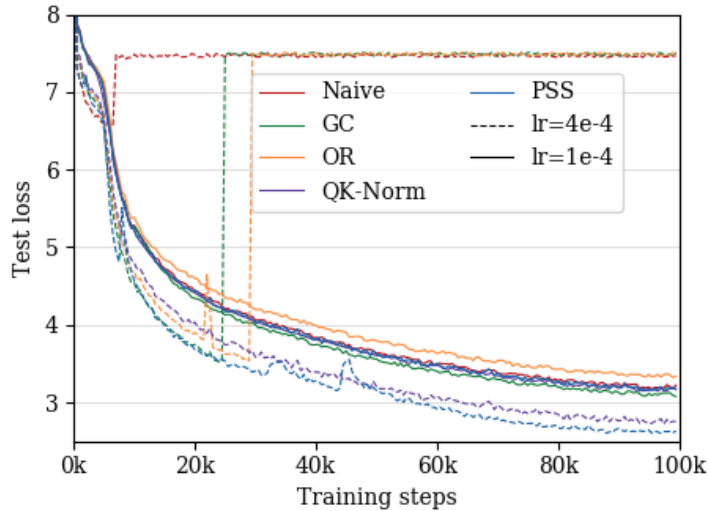


Figure 4: Loss curves with different stabilization methods.

D.3 Experiment Results on Larger Models

We validated the effectiveness of our method on larger models, including BERT-large (340M), GPT-2-Large (774M), and GPT-2-XL (1.5B). For these larger models, we primarily compared with the naive baseline to demonstrate our method’s ability to stabilize training (see table 6). In all three models, we successfully used large learning rates, which would cause instability in the naive baseline, to achieve stable training.

Table 6: Results on BERT-Large, GPT-2-Large, GPT-2-XL and LLaMa3-8B

Method \ Model	BERT-Large		GPT-2-Large		GPT-2-XL		LLaMa3-8B	
	lr=5e-5	lr=1e-4	lr=5e-5	lr=1e-4	lr=1e-5	lr=5e-5	lr=5e-4	lr=1e-3
Naive	0/2 _{2.4±0.1}	2/2	0/1 _{3.9}	1/1	0/1 _{3.7}	1/1	0/2 _{3.8±0.1}	2/2
GC	—	0/2 _{2.9±0.1}	—	0/2 _{5.2±0.3}	—	0/1 _{4.3}	—	—
OR	—	3/3	—	1/1	—	1/1	—	—
QK-Norm	—	0/2 _{2.9±0.2}	—	1/1	—	0/1 _{3.9}	—	—
PSS	0/2 _{2.4±0.1}	0/2 _{2.7±0.1}	0/1 _{4.0}	0/1 _{4.2}	0/1 _{3.8}	0/1 _{3.9}	0/2 _{3.8±0.1}	0/2 _{3.8±0.1}

D.4 Experiment Results on different Hyper-parameters

In addition to the learning rate, we also evaluated the performance of the PSS method under various other hyper-parameter settings. Specifically, we compared the PSS method with the Naive method across different batch sizes (set to 1 and 64) and different learning rate warm-up steps (set to 1 and 1000). The experimental results(see table 7) indicate that the Naive method exhibited instability when the batch size was excessively small (batch size = 1) and when no learning rate warm-up strategy was employed. In contrast, the PSS method demonstrated the capability to maintain stable model training under these conditions.

Table 7: Results on BERT-Large, GPT-2-Large and GPT-2-XL

Method	Hyper-params	Batch Size		LR Warmup Steps	
		64	1	1000	1
Naive	0/3 _{3.0±0.2}	4/4 _{7.5±0.1}	0/3 _{3.0±0.2}	3/3 _{7.5±0.1}	—
GC	—	0/1 _{3.2}	—	0/1 _{3.0}	—
OR	—	0/2 _{4.0±0.1}	—	1/1	—
QK-Norm	—	0/2 _{3.3±0.1}	—	2/2	—
PSS Naive	0/3 _{3.0±0.1}	0/4 _{3.4±0.2}	0/3 _{3.0±0.2}	0/3 _{2.9±0.1}	—

D.5 Experiment Results on PSS Activation Frequency

Table 8: Frequency of PSS activation across different settings on BERT.

Learning Rate	BERT-base		BERT-large	
	@50k step	@100k step	@50k step	@100k step
Small LR	0.02%(lr=1e-4)	0.03%(lr=1e-4)	0.03%(lr=5e-5)	0.03%(lr=5e-5)
Large LR	0.09%(lr=4e-4)	0.06%(lr=4e-4)	0.16%(lr=1e-4)	0.11%(lr=1e-4)

Table 9: Frequency of PSS activation across different settings on GPT-2.

Learning Rate	GPT-2-medium		GPT-2-large	
	@100k step	@200k step	@100k step	@200k step
Small LR	0.05%(lr=5e-4)	0.03%(lr=5e-4)	0.06%(lr=5e-5)	0.05%(lr=5e-5)
Large LR	0.23%(lr=1e-3)	0.15%(lr=1e-3)	0.19%(lr=1e-4)	0.15%(lr=1e-4)

E Empirical Observation

E.1 Observation on Representation Dominance

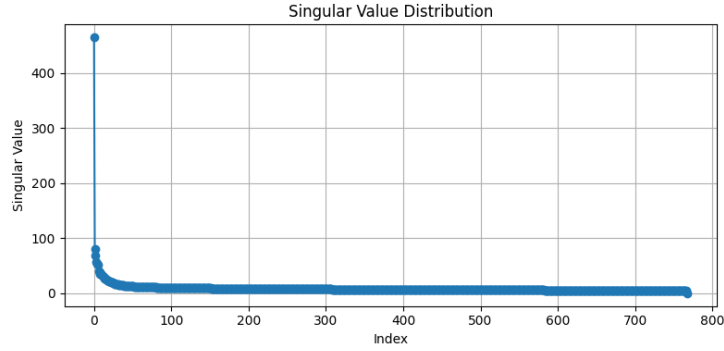


Figure 5: Singular value distribution of the representation matrix in the embedding layer.

E.2 Observation on Different Modules

Below is the evolution of $SR(\mathbf{W})$, $SR(\mathbf{Z})$, singularity alignment ϕ , and the combined representation of training loss and gradient norm across the Attention Key, Query, value matrix, and FFN Dense 1 module.

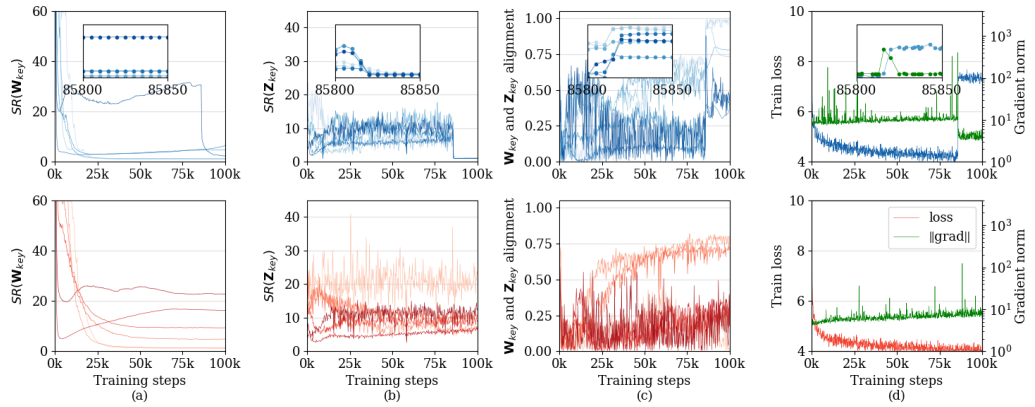


Figure 6: Observation on Attention Key matrix.

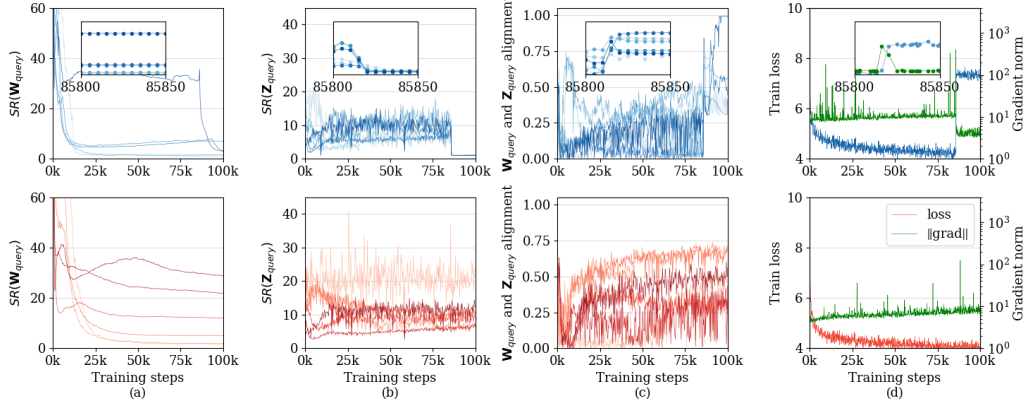


Figure 7: Observation on Attention Query matrix.

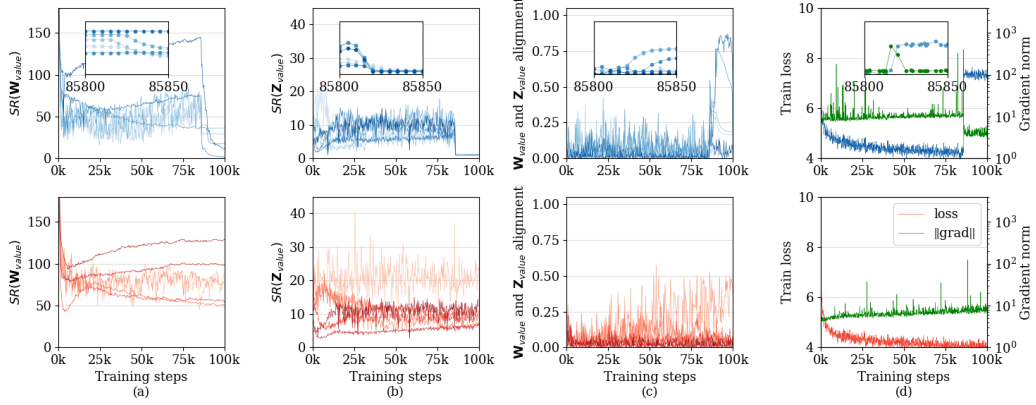


Figure 8: Observation on Attention Value matrix.

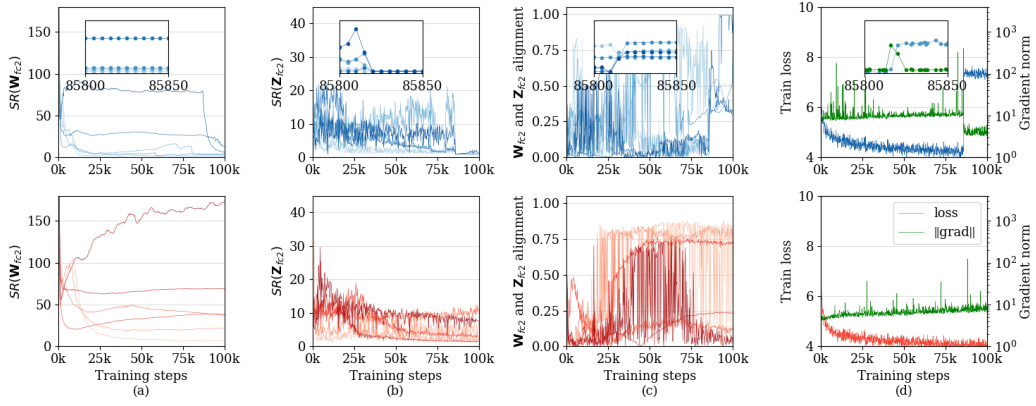


Figure 9: Observation on FFN Dense 1 module.

F Limitation Discussion

A key limitation is the absence of validation on industrial-scale models and proprietary datasets.

NeurIPS Paper Checklist

1. Claims

Question: Do the main claims made in the abstract and introduction accurately reflect the paper's contributions and scope?

Answer: [\[Yes\]](#)

Justification: All the claims made in abstract and introduction reflect the paper's contributions and insight clearly.

Guidelines:

- The answer NA means that the abstract and introduction do not include the claims made in the paper.
- The abstract and/or introduction should clearly state the claims made, including the contributions made in the paper and important assumptions and limitations. A No or NA answer to this question will not be perceived well by the reviewers.
- The claims made should match theoretical and experimental results, and reflect how much the results can be expected to generalize to other settings.
- It is fine to include aspirational goals as motivation as long as it is clear that these goals are not attained by the paper.

2. Limitations

Question: Does the paper discuss the limitations of the work performed by the authors?

Answer: [\[Yes\]](#)

Justification: See appendix F.

Guidelines:

- The answer NA means that the paper has no limitation while the answer No means that the paper has limitations, but those are not discussed in the paper.
- The authors are encouraged to create a separate "Limitations" section in their paper.
- The paper should point out any strong assumptions and how robust the results are to violations of these assumptions (e.g., independence assumptions, noiseless settings, model well-specification, asymptotic approximations only holding locally). The authors should reflect on how these assumptions might be violated in practice and what the implications would be.
- The authors should reflect on the scope of the claims made, e.g., if the approach was only tested on a few datasets or with a few runs. In general, empirical results often depend on implicit assumptions, which should be articulated.
- The authors should reflect on the factors that influence the performance of the approach. For example, a facial recognition algorithm may perform poorly when image resolution is low or images are taken in low lighting. Or a speech-to-text system might not be used reliably to provide closed captions for online lectures because it fails to handle technical jargon.
- The authors should discuss the computational efficiency of the proposed algorithms and how they scale with dataset size.
- If applicable, the authors should discuss possible limitations of their approach to address problems of privacy and fairness.
- While the authors might fear that complete honesty about limitations might be used by reviewers as grounds for rejection, a worse outcome might be that reviewers discover limitations that aren't acknowledged in the paper. The authors should use their best judgment and recognize that individual actions in favor of transparency play an important role in developing norms that preserve the integrity of the community. Reviewers will be specifically instructed to not penalize honesty concerning limitations.

3. Theory assumptions and proofs

Question: For each theoretical result, does the paper provide the full set of assumptions and a complete (and correct) proof?

Answer: [\[Yes\]](#)

Justification: See analysis 2 and theoretical proof A.

Guidelines:

- The answer NA means that the paper does not include theoretical results.
- All the theorems, formulas, and proofs in the paper should be numbered and cross-referenced.
- All assumptions should be clearly stated or referenced in the statement of any theorems.
- The proofs can either appear in the main paper or the supplemental material, but if they appear in the supplemental material, the authors are encouraged to provide a short proof sketch to provide intuition.
- Inversely, any informal proof provided in the core of the paper should be complemented by formal proofs provided in appendix or supplemental material.
- Theorems and Lemmas that the proof relies upon should be properly referenced.

4. Experimental result reproducibility

Question: Does the paper fully disclose all the information needed to reproduce the main experimental results of the paper to the extent that it affects the main claims and/or conclusions of the paper (regardless of whether the code and data are provided or not)?

Answer: **[Yes]**

Justification: We fully demonstrate our method and experiment settings in section 3 and section 4.1. See more details in appendix C.1 and appendix D.1

Guidelines:

- The answer NA means that the paper does not include experiments.
- If the paper includes experiments, a No answer to this question will not be perceived well by the reviewers: Making the paper reproducible is important, regardless of whether the code and data are provided or not.
- If the contribution is a dataset and/or model, the authors should describe the steps taken to make their results reproducible or verifiable.
- Depending on the contribution, reproducibility can be accomplished in various ways. For example, if the contribution is a novel architecture, describing the architecture fully might suffice, or if the contribution is a specific model and empirical evaluation, it may be necessary to either make it possible for others to replicate the model with the same dataset, or provide access to the model. In general, releasing code and data is often one good way to accomplish this, but reproducibility can also be provided via detailed instructions for how to replicate the results, access to a hosted model (e.g., in the case of a large language model), releasing of a model checkpoint, or other means that are appropriate to the research performed.
- While NeurIPS does not require releasing code, the conference does require all submissions to provide some reasonable avenue for reproducibility, which may depend on the nature of the contribution. For example
 - (a) If the contribution is primarily a new algorithm, the paper should make it clear how to reproduce that algorithm.
 - (b) If the contribution is primarily a new model architecture, the paper should describe the architecture clearly and fully.
 - (c) If the contribution is a new model (e.g., a large language model), then there should either be a way to access this model for reproducing the results or a way to reproduce the model (e.g., with an open-source dataset or instructions for how to construct the dataset).
 - (d) We recognize that reproducibility may be tricky in some cases, in which case authors are welcome to describe the particular way they provide for reproducibility. In the case of closed-source models, it may be that access to the model is limited in some way (e.g., to registered users), but it should be possible for other researchers to have some path to reproducing or verifying the results.

5. Open access to data and code

Question: Does the paper provide open access to the data and code, with sufficient instructions to faithfully reproduce the main experimental results, as described in supplemental material?

Answer: **[No]**

Justification: We will fully release our code if this paper was accepted.

Guidelines:

- The answer NA means that paper does not include experiments requiring code.
- Please see the NeurIPS code and data submission guidelines (<https://nips.cc/public/guides/CodeSubmissionPolicy>) for more details.
- While we encourage the release of code and data, we understand that this might not be possible, so “No” is an acceptable answer. Papers cannot be rejected simply for not including code, unless this is central to the contribution (e.g., for a new open-source benchmark).
- The instructions should contain the exact command and environment needed to run to reproduce the results. See the NeurIPS code and data submission guidelines (<https://nips.cc/public/guides/CodeSubmissionPolicy>) for more details.
- The authors should provide instructions on data access and preparation, including how to access the raw data, preprocessed data, intermediate data, and generated data, etc.
- The authors should provide scripts to reproduce all experimental results for the new proposed method and baselines. If only a subset of experiments are reproducible, they should state which ones are omitted from the script and why.
- At submission time, to preserve anonymity, the authors should release anonymized versions (if applicable).
- Providing as much information as possible in supplemental material (appended to the paper) is recommended, but including URLs to data and code is permitted.

6. Experimental setting/details

Question: Does the paper specify all the training and test details (e.g., data splits, hyper-parameters, how they were chosen, type of optimizer, etc.) necessary to understand the results?

Answer: **[Yes]**

Justification: See 4.1

Guidelines:

- The answer NA means that the paper does not include experiments.
- The experimental setting should be presented in the core of the paper to a level of detail that is necessary to appreciate the results and make sense of them.
- The full details can be provided either with the code, in appendix, or as supplemental material.

7. Experiment statistical significance

Question: Does the paper report error bars suitably and correctly defined or other appropriate information about the statistical significance of the experiments?

Answer: **[Yes]**

Justification: See table 1 and table 2 for example.

Guidelines:

- The answer NA means that the paper does not include experiments.
- The authors should answer “Yes” if the results are accompanied by error bars, confidence intervals, or statistical significance tests, at least for the experiments that support the main claims of the paper.
- The factors of variability that the error bars are capturing should be clearly stated (for example, train/test split, initialization, random drawing of some parameter, or overall run with given experimental conditions).
- The method for calculating the error bars should be explained (closed form formula, call to a library function, bootstrap, etc.)
- The assumptions made should be given (e.g., Normally distributed errors).
- It should be clear whether the error bar is the standard deviation or the standard error of the mean.

- It is OK to report 1-sigma error bars, but one should state it. The authors should preferably report a 2-sigma error bar than state that they have a 96% CI, if the hypothesis of Normality of errors is not verified.
- For asymmetric distributions, the authors should be careful not to show in tables or figures symmetric error bars that would yield results that are out of range (e.g. negative error rates).
- If error bars are reported in tables or plots, The authors should explain in the text how they were calculated and reference the corresponding figures or tables in the text.

8. Experiments compute resources

Question: For each experiment, does the paper provide sufficient information on the computer resources (type of compute workers, memory, time of execution) needed to reproduce the experiments?

Answer: [\[Yes\]](#)

Justification: All the experiment results are conducted with 8 A100 GPUs.

Guidelines:

- The answer NA means that the paper does not include experiments.
- The paper should indicate the type of compute workers CPU or GPU, internal cluster, or cloud provider, including relevant memory and storage.
- The paper should provide the amount of compute required for each of the individual experimental runs as well as estimate the total compute.
- The paper should disclose whether the full research project required more compute than the experiments reported in the paper (e.g., preliminary or failed experiments that didn't make it into the paper).

9. Code of ethics

Question: Does the research conducted in the paper conform, in every respect, with the NeurIPS Code of Ethics <https://neurips.cc/public/EthicsGuidelines>?

Answer: [\[Yes\]](#)

Justification: Yes, we claim the research conducted in the paper conform, in every respect, with the NeurIPS Code of Ethics.

Guidelines:

- The answer NA means that the authors have not reviewed the NeurIPS Code of Ethics.
- If the authors answer No, they should explain the special circumstances that require a deviation from the Code of Ethics.
- The authors should make sure to preserve anonymity (e.g., if there is a special consideration due to laws or regulations in their jurisdiction).

10. Broader impacts

Question: Does the paper discuss both potential positive societal impacts and negative societal impacts of the work performed?

Answer: [\[NA\]](#)

Justification: The paper does not appear to discuss potential positive or negative societal impacts of the work, as it emphasizes a technical advancement without addressing broader societal implications.

Guidelines:

- The answer NA means that there is no societal impact of the work performed.
- If the authors answer NA or No, they should explain why their work has no societal impact or why the paper does not address societal impact.
- Examples of negative societal impacts include potential malicious or unintended uses (e.g., disinformation, generating fake profiles, surveillance), fairness considerations (e.g., deployment of technologies that could make decisions that unfairly impact specific groups), privacy considerations, and security considerations.

- The conference expects that many papers will be foundational research and not tied to particular applications, let alone deployments. However, if there is a direct path to any negative applications, the authors should point it out. For example, it is legitimate to point out that an improvement in the quality of generative models could be used to generate deepfakes for disinformation. On the other hand, it is not needed to point out that a generic algorithm for optimizing neural networks could enable people to train models that generate Deepfakes faster.
- The authors should consider possible harms that could arise when the technology is being used as intended and functioning correctly, harms that could arise when the technology is being used as intended but gives incorrect results, and harms following from (intentional or unintentional) misuse of the technology.
- If there are negative societal impacts, the authors could also discuss possible mitigation strategies (e.g., gated release of models, providing defenses in addition to attacks, mechanisms for monitoring misuse, mechanisms to monitor how a system learns from feedback over time, improving the efficiency and accessibility of ML).

11. Safeguards

Question: Does the paper describe safeguards that have been put in place for responsible release of data or models that have a high risk for misuse (e.g., pretrained language models, image generators, or scraped datasets)?

Answer: [NA]

Justification: The paper does not release data or models that could pose a high risk for misuse.

Guidelines:

- The answer NA means that the paper poses no such risks.
- Released models that have a high risk for misuse or dual-use should be released with necessary safeguards to allow for controlled use of the model, for example by requiring that users adhere to usage guidelines or restrictions to access the model or implementing safety filters.
- Datasets that have been scraped from the Internet could pose safety risks. The authors should describe how they avoided releasing unsafe images.
- We recognize that providing effective safeguards is challenging, and many papers do not require this, but we encourage authors to take this into account and make a best faith effort.

12. Licenses for existing assets

Question: Are the creators or original owners of assets (e.g., code, data, models), used in the paper, properly credited and are the license and terms of use explicitly mentioned and properly respected?

Answer: [Yes]

Justification: We have cited the original owners of assets in this paper.

Guidelines:

- The answer NA means that the paper does not use existing assets.
- The authors should cite the original paper that produced the code package or dataset.
- The authors should state which version of the asset is used and, if possible, include a URL.
- The name of the license (e.g., CC-BY 4.0) should be included for each asset.
- For scraped data from a particular source (e.g., website), the copyright and terms of service of that source should be provided.
- If assets are released, the license, copyright information, and terms of use in the package should be provided. For popular datasets, paperswithcode.com/datasets has curated licenses for some datasets. Their licensing guide can help determine the license of a dataset.
- For existing datasets that are re-packaged, both the original license and the license of the derived asset (if it has changed) should be provided.

- If this information is not available online, the authors are encouraged to reach out to the asset's creators.

13. New assets

Question: Are new assets introduced in the paper well documented and is the documentation provided alongside the assets?

Answer: [NA]

Justification: The paper does not release new assets.

Guidelines:

- The answer NA means that the paper does not release new assets.
- Researchers should communicate the details of the dataset/code/model as part of their submissions via structured templates. This includes details about training, license, limitations, etc.
- The paper should discuss whether and how consent was obtained from people whose asset is used.
- At submission time, remember to anonymize your assets (if applicable). You can either create an anonymized URL or include an anonymized zip file.

14. Crowdsourcing and research with human subjects

Question: For crowdsourcing experiments and research with human subjects, does the paper include the full text of instructions given to participants and screenshots, if applicable, as well as details about compensation (if any)?

Answer: [NA]

Justification: The paper does not involve crowdsourcing nor research with human subjects.

Guidelines:

- The answer NA means that the paper does not involve crowdsourcing nor research with human subjects.
- Including this information in the supplemental material is fine, but if the main contribution of the paper involves human subjects, then as much detail as possible should be included in the main paper.
- According to the NeurIPS Code of Ethics, workers involved in data collection, curation, or other labor should be paid at least the minimum wage in the country of the data collector.

15. Institutional review board (IRB) approvals or equivalent for research with human subjects

Question: Does the paper describe potential risks incurred by study participants, whether such risks were disclosed to the subjects, and whether Institutional Review Board (IRB) approvals (or an equivalent approval/review based on the requirements of your country or institution) were obtained?

Answer: [NA]

Justification: The paper does not involve crowdsourcing nor research with human subjects.

Guidelines:

- The answer NA means that the paper does not involve crowdsourcing nor research with human subjects.
- Depending on the country in which research is conducted, IRB approval (or equivalent) may be required for any human subjects research. If you obtained IRB approval, you should clearly state this in the paper.
- We recognize that the procedures for this may vary significantly between institutions and locations, and we expect authors to adhere to the NeurIPS Code of Ethics and the guidelines for their institution.
- For initial submissions, do not include any information that would break anonymity (if applicable), such as the institution conducting the review.

16. Declaration of LLM usage

Question: Does the paper describe the usage of LLMs if it is an important, original, or non-standard component of the core methods in this research? Note that if the LLM is used only for writing, editing, or formatting purposes and does not impact the core methodology, scientific rigorosity, or originality of the research, declaration is not required.

Answer: [NA]

Justification: The core method development in this research does not involve LLMs as any important, original, or non-standard components.

Guidelines:

- The answer NA means that the core method development in this research does not involve LLMs as any important, original, or non-standard components.
- Please refer to our LLM policy (<https://neurips.cc/Conferences/2025/LLM>) for what should or should not be described.